NIST Technical Note 1492

Acoustic Sensing of Hydrating Cement Suspensions: An Exploratory Study

Vincent A. Hackley
Lin-Sien Lum
Chiara F. Ferraris

NIST National Institute of Standards and Technology • U.S. Department of Commerce

NIST Technical Note 1492

Acoustic Sensing of Hydrating Cement Suspensions: An Exploratory Study

Vincent A. Hackley
Lin-Sien Lum
Ceramics Division
Materials Science & Engineering Laboratory

Chiara F. Ferraris
Materials & Construction Research Division
Building & Fire Research Laboratory

December 2007

U.S. Department of Commerce
Carlos M. Gutierrez, Secretary

National Institute of Standards and Technology
James M. Turner, Acting Director

National Institute of Standards and Technology Technical Publication 1492
Natl. Inst. Stand. Technol. Tech. Publ. 1492, 35 pages (December 2007)
CODEN: NSPUE2

U.S. GOVERNMENT PRINTING OFFICE
WASHINGTON: 2007

For sale by the Superintendent of Documents, U.S. Government Printing Office
Internet: bookstore.gpo.gov — Phone: (202) 512-1800 — Fax: (202) 512-2250
Mail: Stop SSOP, Washington, DC 20402-0001

Acoustic Sensing of Hydrating Cement Suspensions: An Exploratory Study

1. Introduction

Portland cement is a complex heterogeneous mixture of mineral phases, all of which react with water to varying degrees and at different rates. The principal components are tricalcium silicate (Ca_3SiO_5: C_3S), β dicalcium silicate (Ca_2SiO_4: C_2S), tricalcium aluminate ($Ca_3Al_2O_6$: C_3A) and tetracalcium aluminoferrite ($Ca_4Al_2Fe_2O_{10}$: C_4AF).[1] Of these, the calcium silicates C_3S and C_2S are the main constituents responsible for the setting of portland cement. Their principal hydration product is calcium silicate hydrate (C-S-H), a mostly amorphous phase that forms at the surface of cement particles and in the interstitial fluid. C-S-H is not a well defined material; it can vary chemically depending on the exact composition of the starting powder as well as other factors. Morphologically, C-S-H remains largely unresolved, although recent studies have determined that the primary dimension of the hydrate product lies in the nanoscale range with specific surface areas varying widely from a few tens of m^2/g up to 1000 m^2/g or thereabouts [2,3].

Upon contact with an aqueous phase, cement powder begins a complicated process that leads over time to a hardened solid. During roughly the first 2 h after contact, the initial hydrolysis of calcium silicates and dissolution of ions occurs. Following the dormant period during which the ion concentration steadily increases, the initial formation of C-S-H products occurs in the acceleration period. Hydration reaches a maximum rate about (4 to 8) h following initial contact with water, and continues to decrease for several days afterward. The kinetics of hydration are dependent on a number of factors, including the cement particle size distribution (PSD) [4], cement/water ratio and impurities [1], and the addition of chemical admixtures (accelerants and retardants) [5-7].

In addition to flow and mechanical property measurements, such as yield stress, numerous ex situ approaches have been applied to the study of cement hydration during early times (i.e., a few minutes to several hours after contact with water), including pH and conductivity measurements, X-ray diffraction, nitrogen adsorption, electron spectroscopy for chemical analysis (ESCA), inductively coupled plasma emission (ICP), and scanning electron microscopy (SEM) [2,8-12]. Several in situ techniques have also been explored recently to investigate the hydration process, in particular thermal analysis [5,6,13-19], electrical impedance [20,21], nuclear magnetic resonance (NMR) [22,23], neutron scattering [3,24-27], small-angle x-ray scattering (SAXS) [28], and X-ray computed tomography (CT) [29,30].

By comparison, ultrasonic-based techniques have found broad application in the non-destructive in situ characterization of cement. Ultrasonics uses high-frequency sound waves to penetrate the cement material and interstitial pore solution, and can provide information on the elastic and viscoelastic properties and their characteristic moduli. Although the use of sound waves has been of particular interest in the characterization of hardened cements, due to the relationship between sound propagation and the mechanical properties of elastic solids [31,32], the analysis of early age hydration in pastes and suspensions using ultrasonics has grown rapidly in recent years [19,29,33-65]. The propagation of compressional waves in a porous elastic solid saturated by a viscous fluid has been treated by Biot [66,67], and most applications of compressional ultrasonic waves in cement systems draw on Biot's theoretical framework to interpret experimental results.

Ultrasonic techniques applied to the study of early age hydration can be differentiated by whether they use transmission or reflectance mode detection, and whether compression or shear waves are applied. Shear waves only propagate in solids, while compression waves propagate in solids, liquids and gases. Thus shear waves are especially sensitive to the onset of hardening or network percolation. A round-robin comparison of compressive wave and shear wave measurements, as applied to the study of the setting of cement, has been published recently by Voigt et al.[62].

In the majority of cases, the experimental apparatus makes use of a pulse (i.e., tone burst), rather than continuous wave transducer, with nominal center frequencies typically in the 100 kHz to 10 MHz range. Measurements most often focus on sound speed variation over time [19,34,35,41,45-47,51-55,64,65], but attenuation and impedance (reflection coefficient) measurements have also been widely reported [33-35,41,45,48,50,53,56,57,59-61,63]. The most commonly utilized acoustic set-up for cement hydration/setting relies on the *pulse echo* technique, in which velocity (based on transit time), attenuation, and impedance can all be determined using a single transducer as source and detector. Other methods include: *acoustic emission* [36-38], a passive technique, *acoustic near field* [39,40,43,49], which is sensitive to the mechanical loading exerted on an immersed resonator tip, and *electroacoustics* (i.e., acoustophoresis and electroacoustic sonic amplitude - ESA) [42,44], which are sensitive to the electrokinetic (zeta) potential of cement particles. Few reported studies have examined the frequency-dependence of acoustic attenuation or velocity measurements in hydrating cement. In addition, no published work, to our knowledge, has explored the frequency domain above 10 MHz.

In this technical note we summarize preliminary results from an exploratory investigation to examine the application of high-frequency acoustic spectroscopy in the study of early age cement hydration. In particular, we are interested in detecting and monitoring the initial nanoscale C-S-H product formed in cement slurries prepared at relatively high water/cement (w/c) mass ratios, and the effect of chemical admixtures on this process.

2. Acoustic Sensing

In the context of the present work, acoustic sensing refers to the application of radio-frequency sound waves to monitor changes in certain physical characteristics of non-dilute particulate suspensions [68-70]. When compressive (longitudinal) sound waves propagate in such a material, they experience "excess" attenuation (identified by the symbol α) due to the presence of the dispersed phase.

Viscous attenuation results from relative motion between the particle and adjacent liquid layers as the oscillating sound wave crosses the solid-liquid interface. This motion is induced by differences in density between the two phases. The viscous drag of the medium and the nonpropagating shear wave generated by the relative motion act to dissipate part of the sound wave energy as it passes. Particle inertia also dampens the motion and thereby dissipates energy, though very small particles (< 100 nm) exhibit negligible inertial effects. For viscous attenuation, a critical frequency, f_c, can be defined such that [71,72]:

$$f_c = \frac{9}{4\pi} \cdot \frac{\eta}{a^2 \rho_s}$$

where η is the liquid phase viscosity, ρ_s is the particle bulk density and a is the particle radius. This is the frequency of maximum attenuation due to viscous loss, and it is seen to increase as the particle size decreases. It also increases with fluid viscosity and decreases with increasing particle density. Viscous loss typically produces a bell shaped attenuation spectrum, with the maximum at f_c. Sensitivity to changes in the dispersed phase is maximal in the vicinity of the critical frequency.

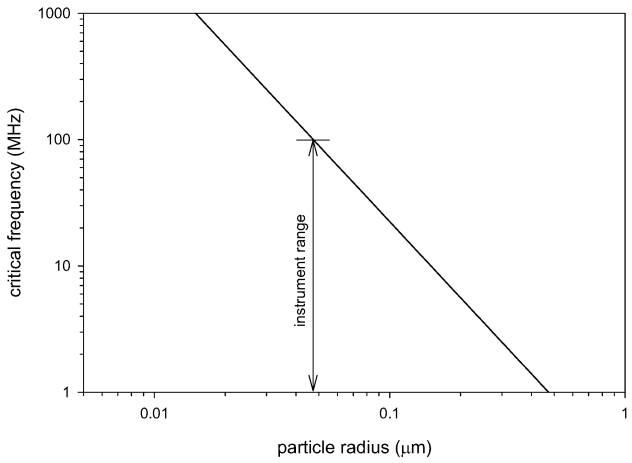

Fig. 1 Critical frequency for viscous attenuation in water at 20 º as a function of particle size, calculated using a density of 3.2 g/cm^3 appropriate for Portland cement).

So-called *visco-inertial* losses are the principal mechanism of attenuation by rigid colloidal-sized particles in high density contrast† media [72].

Another loss mechanism to consider is scattering, where the sound waves are redirected away from the detector by the presence of the particles, much in the same way that light waves are scattered. Scattering is a strong function of frequency and size, and for the long-wavelength regime [73]:

$$\alpha_{scattering} \sim \frac{f^4 a^3}{V_f}$$

As particle size increases relative to the wavelength of sound ($\lambda \approx 1.5$ mm in water at 1 MHz), acoustic scattering becomes an important loss mechanism, and in the (1 to 100) MHz range it can be a fairly significant source of attenuation for particles greater than about 3 μm. It can be largely ignored for colloidal suspensions. The presence of scattering is indicated by an increase in attenuation at frequencies well above the critical frequency for visco-inertial loss, producing an attenuation minimum (see Fig. 2, e.g.).

The other important loss mechanism for high contrast suspensions is "intrinsic" or bulk molecular attenuation, which depends on the volume fraction of each phase present, and is not affected by the form or domain size of the material. Intrinsic losses for the dispersed phase are generally very small and can often be ignored, and hence the suspension intrinsic loss is typically dominated by the medium. Thermal loss mechanisms, important for emulsions and latex suspensions, need not be considered for high density contrast suspensions. Losses due to viscous, scattering, and intrinsic attenuation are treated as additive.

Figure 2 shows the theoretically calculated spectra in water for rigid spheres with radius 1 μm, 0.3 μm and 0.05 μm. The density contrast is set to 2. Calculations are based on a version of

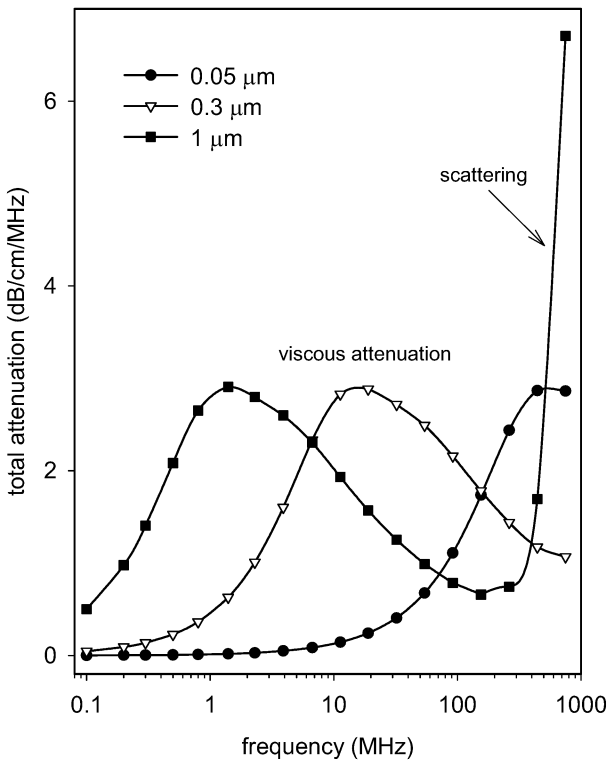

Fig. 2. Attenuation spectra calculated for monodisperse rigid particles of different radii in water. Parameters used in calculation: volume fraction is 5 %, density contrast is 2, temperature is 20 ºC.

† Density contrast refers to the difference in bulk density between the dispersed solid phase and suspending medium. Systems in which $\Delta\rho$ is significantly greater than 1 are referred to as high density contrast.

the coupled-phase model as described by Dukhin and Goetz [72,74]. A shift in the critical frequency for viscous attenuation with particle size can be clearly seen, and the onset of scattering losses at high frequencies is evident for the largest particle size. As Fig. 2 suggests, particles in the nanosize regime should exhibit significant attenuation only at high frequencies.

For a given suspension, the total measured attenuation spectra will depend on a number of factors, including solids loading, particle size relative to the acoustic wavelength, density contrast, and the viscosity of the suspending medium. By measuring the attenuation spectra over a range of frequencies, information about the microstructure of the dispersed phase can be extracted using a suitable model, or inferred on the basis of a reasonable physical description of the system coupled with a knowledge of the predominant underlying loss mechanism(s).

A commercially available acoustic spectrometer (see section 3 for a full description) was utilized in the present work. This instrument uses a pulse-wave technique in which sound pulses generated at the surface of one transducer, are transmitted through the sample, and are detected by a second transducer. The sound energy loss (attenuation) and sound velocity (at a single frequency) are measured. A frequency range from (1 to 100) MHz is scanned by varying the gap distance between the transmitter and receiver. The sensor design is sufficiently robust to handle flowing suspensions with solid volume fractions exceeding 35 %, and alkaline environments such as those typically associated with hydrating cement slurries. Based on feedback from our research, modifications were made by the manufacturer to improve the overall performance of the instrument for cement applications, including a better method for sealing the moving source transducer in contact with the cement slurry. The energy of the sound used in the acoustic spectrometer is too low to impact suspension microstructure, and therefore the technique is considered to be *non-destructive*.

The acoustic spectrometer can process measured attenuation spectra to produce particle size distributions using a modified *coupled-phase* model that accounts for interparticle hydrodynamic effects at high solids concentrations [68,72]. This approach was not used in the present work due to the inherent complexity of portland cement. The coupled-phase theory is most applicable when the visco-inertial mechanism dominates the energy loss spectrum, the size distribution is relatively simple (e.g., the analysis algorithm assumes a log-normal function), and the particle phase is homogeneous and characterized by a spherical morphology. Clearly, portland cement powder, with it's variable and asymmetric morphology, extreme size polydispersity, and heterogeneous mineral phase, does not closely conform to the physical reality of this or any other known acoustic model. Additionally, the prevalence of micrometer-size particles in portland cement (upwards of 100 μm diameter) leads to a significant energy loss from acoustic scattering, which complicates the attenuation spectra over the high frequency range.

Instead, we employ a simple phenomenological approach, in which excess attenuation, expressed in dB/cm/MHz (normalized to the frequency of the sound wave and the emitter-detector distance), is employed as a "soft sensor" for detecting relative physical changes in the suspension. The decibel (dB) is a dimensionless unit describing loss of acoustic intensity and referenced to, in this case, the initial intensity of the acoustic pulse prior to transversing the sample. We then attempt to correlate these changing signals with other physicochemical data on the material under similar conditions. In this manner, we used penetrating high-frequency sound to probe the early stage of hydration (up to roughly 7 h) in cement slurries at solid volume fractions ranging from (2 to 20) %. This corresponds to a minimum w/c of about 1.25. Therefore the slurries studied here remain fluid throughout the test period and formation of network structure is absent, thus allowing us to isolate the C-S-H product formation from the

complexities associated with interparticle bridging and percolation.

The principal advantage of acoustic spectroscopy is its ability to provide reliable information on the physical properties of particles in dense opaque systems. Another advantage is its relative insensitivity to changes in the ionic and electrochemical balance of the system. For the most part, only changes in the physical characteristics, such as particle size, concentration, and interparticle structure, will modify the high-frequency attenuation spectrum of a suspension. Processes such as agglomeration, dissolution and precipitation, which lead to changes in the physical arrangement and dimensions of the solid phase, can be followed using acoustics, even in complex compositions where multiple attenuating species may exist, so long as the other attenuating species remain largely unchanged physically. In this case, an *effective medium* approach can be used to simplify a complex system, with attenuation by non-interactive species lumped into a background signal and subtracted or normalized out. The excess attenuation is then reflective of the interacting or physically evolving species only.

For a more comprehensive treatment of the theoretical aspects of fluid-mediated ultrasonic measurements, and their application for the characterization of particulate suspensions and emulsions, the reader is referred to the recent texts by Povey [75] and Dukhin and Goetz [74], the review published by McClements [69], and the collection of articles edited by Hackley and Texter [76] and derived from the international workshop on *Ultrasonic and Dielectric Characterization Techniques for Suspended Particulates*, held at NIST in 1997.

3. Methods and Materials

A Type I/II ordinary portland cement (CCRL 133) with a Blaine fineness of about 350 m^2/kg was obtained from the Cement and Concrete Reference Laboratory (CCRL) at NIST [77]. Chemical composition and physical property proficiency testing results for CCRL 133 are summarized in Appendix A. Figure 3 shows a

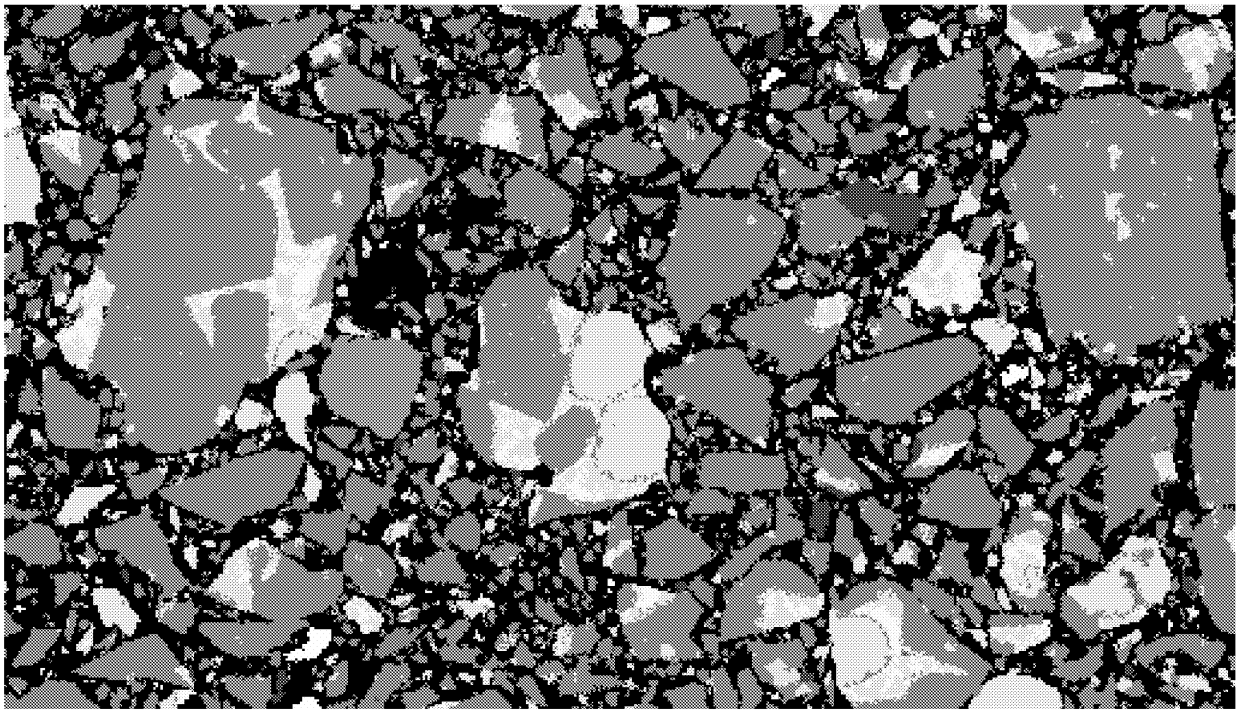

Fig. 3. Gray-scale version of a colorized 2D image of CCRL 133 (500x magnification - 256 μm by 200 μm). Dark gray areas are predominantly C_3S, while lighter shades include C_2S, C_3A, and C_4AF. Original unaltered image available from the VCCTL Cement Images Database at http://ciks.cbt.nist.gov/vcctl/.

gray-scale 2D image of CCRL 133 at 500× magnification. Detailed information on the size and 3-D shape of CCRL 133 cement particles has been published by Garboczi and Bullard[78] based on the use of X-ray microtomographic images.

Six different chemical admixture formulations (high range water reducer admixtures or HRWRAs) were used in this study, including four sulfonate-based and two carboxylate-based. For purposes of this report, the six formulations are identified in Table 1 only by an assigned ID and the chemical class to which each belongs.

Table 1. Chemical admixtures used in study.

ID	Chemical Class
NS1	naphthalene sulfonate
NS2	naphthalene sulfonate
LS	lignosulfonate
MFS	melamine formaldehyde sulfonate
PC1	polycarboxylate
PC2	polycarboxylate

The two polycarboxylates in Table 1 differ in their side-chain length (PC2 has longer side chains), according to the manufacturer. The naphthalene sulfonates NS1 and NS2 are from different manufacturers. Admixtures were provided as a courtesy by W.R. Grace (Construction Products Division, Cambridge, MA) and Degussa Construction Chemicals (Master Builders Technology, Cleveland, OH).

Cement suspensions were prepared gravimetrically using a density of 3.15 g/cm^3 for the cement powder. The powder was added to the required amount of ultrapure deionized water (18 MΩ resistance) to obtain the desired final solid volume fraction. For experiments using chemical admixtures, the required amount of admixture concentrate was added to deionized water and stirred for 5 min. Then the cement powder was added. Suspensions were mixed using a magnetic stirrer for 2 min, and then loaded into the sample chamber of the spectrometer. Care was taken to avoid introducing air bubbles, which can interfere with acoustic measurements.

A commercial acoustic spectrometer (DT-1200, Dispersion Technology Inc., Bedford Hills, NY) was utilized for this study. The DT-1200 measures the attenuation and sound speed using a transmission-mode variable-gap tone-burst technique incorporating a pair of piezoelectric transducers located on opposite sides of the sample [74]. The transmitter generates an ultrasound pulse with a given central frequency and incident intensity. The pulse propagates through the sample and its intensity decays due to the interaction with the sample (see Fig. 4). The receiver converts this attenuated pulse back to an electric signal and sends it to the processing electronics for comparison with the initial pulse, yielding the attenuation, α:

$$\alpha\,[\mathrm{dB/cm/MHz}] = \frac{20}{f[\mathrm{MHz}]\,L[\mathrm{cm}]}\log\frac{I_i}{I_t}$$

where I_i is the incident intensity, I_t is the transmitted intensity, f is the sound frequency in MHz and L is the gap distance.

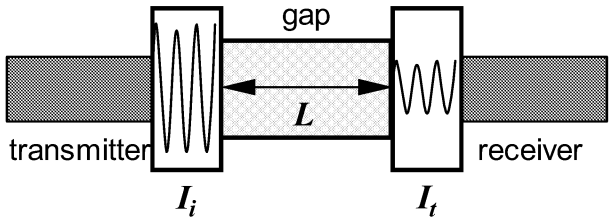

Fig. 4. Schematic layout of transmission mode spectrometer

The receiver is mounted on a piston controlled by a stepping motor that allows the gap between the transmitter and receiver (containing the sample) to be varied systematically. To obtain sufficient signal-to-noise, a minimum of 800 pulses are transmitted for each gap/frequency combination. The reported attenuation is actually determined from the *relative* change in acoustic intensity with a change in gap, so at least two gap distances are required for each

frequency. The adjustable gap allows for a wide dynamic range of frequencies (1 MHz to 100 MHz, typically measured over a logarithmic spacing) and accommodates samples that vary widely in attenuating properties.[†] According to the manufacturer, this frequency range permits characterization of particles as small as 5 nm.

Sound speed in the sample is determined by the ratio of the gap distance, L, to the measured pulse transit time, t:

$$V\,[\mathrm{cm/s}] = \frac{L\,[\mathrm{cm}]}{t\,[\mathrm{s}]}$$

With the DT-1200, sound speed is generally determined only at a single frequency, typically 10 MHz. The group velocity is reported, which represents the speed at which the tone burst envelope propagates through the sample.

Although attenuation spectra are more sensitive to changes in the physical state of the dispersed phase compared with velocity measurements, knowledge of the sound speed facilitates more accurate attenuation measurements in the pulse-transmission technique, and sound speed can be used to determine phase volume changes in some systems.

The reported precision for attenuation measurements using the DT-1200 device is better than 0.1 dB/cm/MHz over the entire frequency range. This result is based on analysis of 10 % mass fraction colloidal silica (Ludox TM50) in water.[74] Sound speed precision determined in the same media is reported to be 0.28 m/s. Also, the manufacturer estimates that the maximum reliably measurable attenuation using the DT-1200 is approximately 390 dB/cm, 600 dB/cm and 1800 dB/cm, for frequencies of 3 MHz, 10 MHz and 100 MHz, respectively. Where error bars are reported, they represent the standard uncertainty (confidence level of approximately 68 %) calculated from replicate measurements.

During experiments, the cement suspensions were continually recirculated through the sample chamber of the spectrometer using an external digital peristaltic pump (Masterflex L/S, Cole-Parmer Instrument Co., Vernon Hills, IL) and food-grade ultra-smooth-bore pump tubing (Masterflex Tygon Food Tubing). Pump rates were varied over a range from (500 to 1000) cm^3/min to determine the potential influence of sample flow on measurements. Most reported data was obtained at a flow rate of either 880 cm^3/min or 1000 cm^3/min, unless otherwise noted.

Intrinsic attenuation due to bulk water was measured separately and subtracted from the attenuation spectra of cement suspensions to yield the excess attenuation due to the cement phase. The time of hydration is determined from the point at which the cement powder first contacted solution. Spectra were recorded beginning shortly after loading the sample, and continued periodically every 30 min for the first (2 to 3) hours, then every 60 min thereafter up to a maximum hydration time of 420 min (7 h). This experimental duration covers most of the

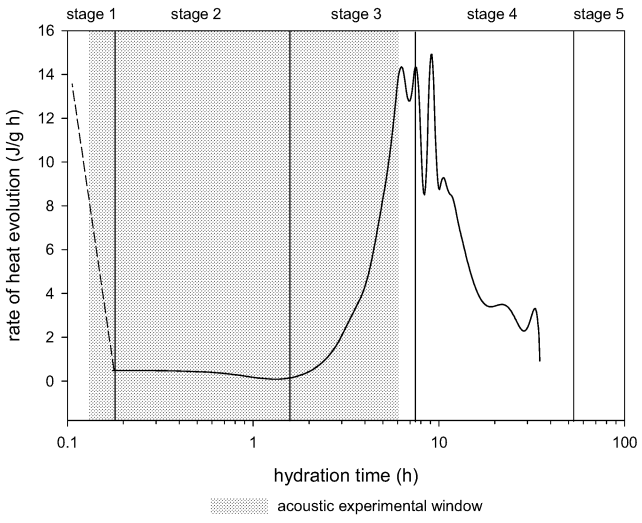

Fig. 5. First derivative of the heat of hydration for CCRL 133 at w/c = 0.45, with the experimental time frame overlaid. Calorimetric data provided by Dale Bentz, NIST-BFRL.

[†] Water is a relatively low attenuating medium. Its attenuation increases linearly with frequency up to 0.2 dB/cm/MHz at 100 MHz.

initial 3 stages of hydration (i.e., initial hydrolysis, dormant period and acceleration) [1]. The experimental window is shown overlaid on the first derivative of the heat of hydration for CCRL 133 in Fig. 5. The approximate demarcations for the various hydration stages are also indicated for convenience. Thermal measurements began during early stage 2, and continued for about 30 h.

In addition to the acoustic sensing elements described above, the spectrometer used for these studies is equipped with a separate sensor for measuring the electroacoustic response to an applied acoustic pulse. The probe, which incorporates a piezoelectric transducer and an electric antenna, are mounted in the flow stream just below the transmitting and receiving transducers used for acoustic spectroscopy.

The theory and principles of colloid vibration current (CVI) and related electroacoustic techniques are detailed elsewhere [68,74,76,79-81]. In brief, for our present application of CVI, a nominal 3 MHz voltage pulse is applied to the emitting transducer. As the acoustic wave propagates through the suspension, it induces a fluctuating motion to charged particles. As a result of this induced motion, the electrical double-layer at the particle-solution interface is displaced periodically relative to the particle. This gives rise to a system of oscillating dipoles, which generate an electrical field that is quantified by measuring the short circuit current. The magnitude of this current is proportional to the charge on the particles.

$$CVI \sim \phi \frac{\Delta\rho}{\rho} \mu(\omega) C_I R_Z$$

where ϕ is the particle volume fraction, $\Delta\rho$ is the density contrast between the particles and suspending fluid, ρ is the fluid density, $\mu(\omega)$ is the frequency dependent dynamic electrophoretic mobility, C_I is an instrument constant that contains device specific terms independent of the test material and requires calibration with a known reference material[82], and R_Z is an acoustic impedance term [83] that can be rolled into the instrumental constant for dilute suspensions but must be determined independently for higher solids loadings.

The zeta potential, ζ, can be calculated from the dynamic mobility according to[80]

$$\mu(\omega) = \frac{\varepsilon\zeta}{\eta} G(\omega)$$

where ε and η are the permittivity and viscosity, of the fluid phase, respectively. The complex frequency-dependent term G reflects the influence of particle inertia on the dynamic mobility. Both magnitude and phase of the response signal depend on particle size. For very small particles (typically less than about 100 nm) or low frequencies, $G = 1$ and inertia is not significant. For larger particles and at higher frequencies, the particle size must be known in order to correct for the effect of inertia and obtain an accurate determination of ζ. For a typical portland cement sample, this correction is impossible to determine as the size distribution of component particles is very broad and the identity of particles that contribute to the measured signal is difficult to clarify. In this case, one can only examine relative changes in the measured electroacoustic response or zeta potential.

An additional complication for electroacoustic analysis of cement is interference from solution electrolytes. The electrolyte load tends to be high for cement suspensions due to dissolution of various species. Ions in solution can and will contribute to the measured electroacoustic response in an additive manner. Typically, this background signal is measured separately for the suspending medium and then subtracted from the sample signal, while also accounting for changes in phase angle. A rough correction method is to simply subtract the two magnitudes without taking phase shifts into consideration. This is problematic for hydrating cement because the ionic composition and concentration in solution are changing with time.

For the scope of the present work, electroacoustic measurements were not of

primary importance, and data is provided simply for informational purposes. No correction has been attempted for either electrolyte background or particle inertia. The electroacoustic sensor was calibrated according to the manufacturer's instructions using a 10 % mass fraction suspension of Ludox TM50 (Aldrich, Milwaukee WI) diluted with 0.01 mol/L KCl. This reference is assigned a value of -38 mV at room temperature.

4. Results and Discussion

Results are presented in their entirety in the hope that future research will benefit from this exploratory study. However, the discussion is limited to that necessary to describe the data as presented. A detailed and complete analysis of the results is left for future peer reviewed publications to address. Here we present in graphical form only the basic results along with essential details that enable the reader to understand the conditions under which the data was obtained. Some conclusions and suggestions for future work are presented in section 5.

Figures 6 to 10 present the frequency-dependent acoustic attenuation and sound speed, and the electroacoustic results obtained for 2 % volume fraction CCRL 133 at different hydration times. This is the lowest solids loading used in these studies. Figures 6 and 7 show the same data set, but in Figure 7 the data has been normalized by subtraction of the spectrum measured at 5 min (which is essentially the starting point for the hydration experiment). This procedure emphasizes the high-frequency "excess" attenuation that increases as hydration proceeds.

Figures 8 and 9 address reproducibility and give results for replicate experiments carried out under identical conditions on different days. Typical coefficients of variation (CV) are observed in the (5 to 20) % range, depending on the measurement frequency. Reproducibility also decreases somewhat at longer hydration times, as one might expect. The precision of replicate measurements on the same sample is difficult to assess due to the time-dependent properties of the hydrating cement, but based on measurements performed on stable suspensions

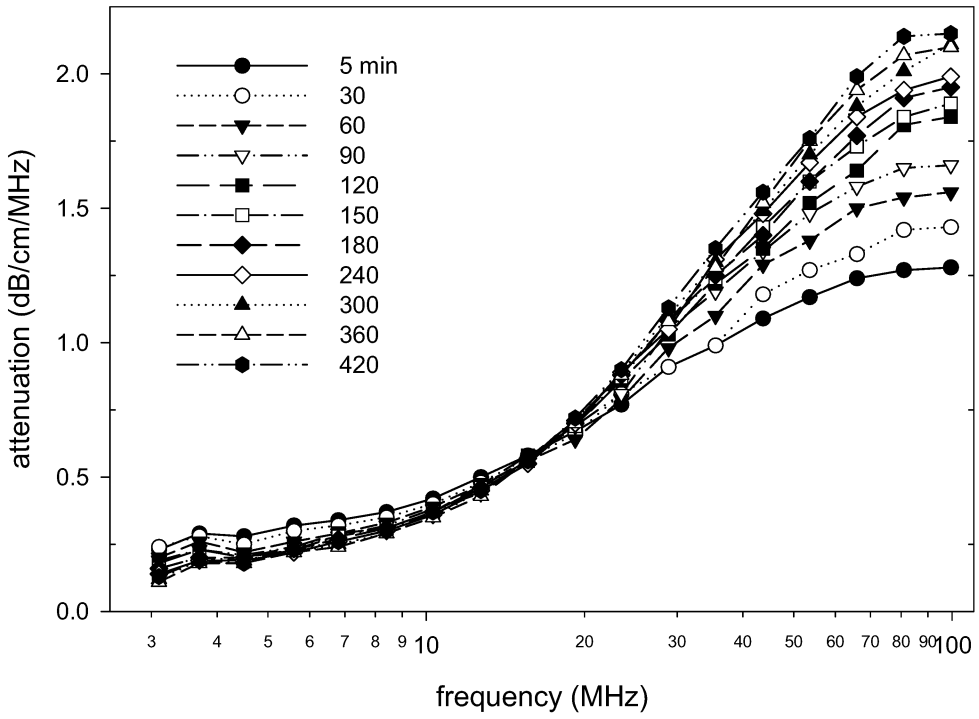

Fig. 6 Evolution of attenuation spectra for 2 % volume fraction CCRL 133 at different hydration times.

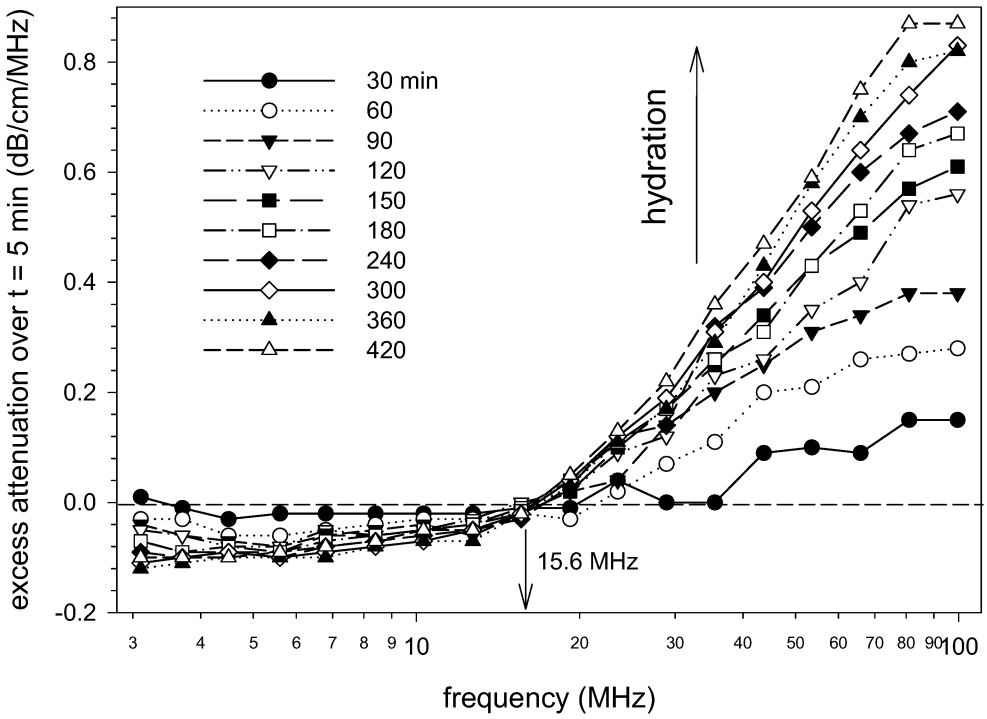

Fig. 7 Excess attenuation after subtraction of t = 5 min spectrum for 2 % volume fraction CCRL 133 at different hydration times. Excess calculated for spectra shown in Fig. 6.

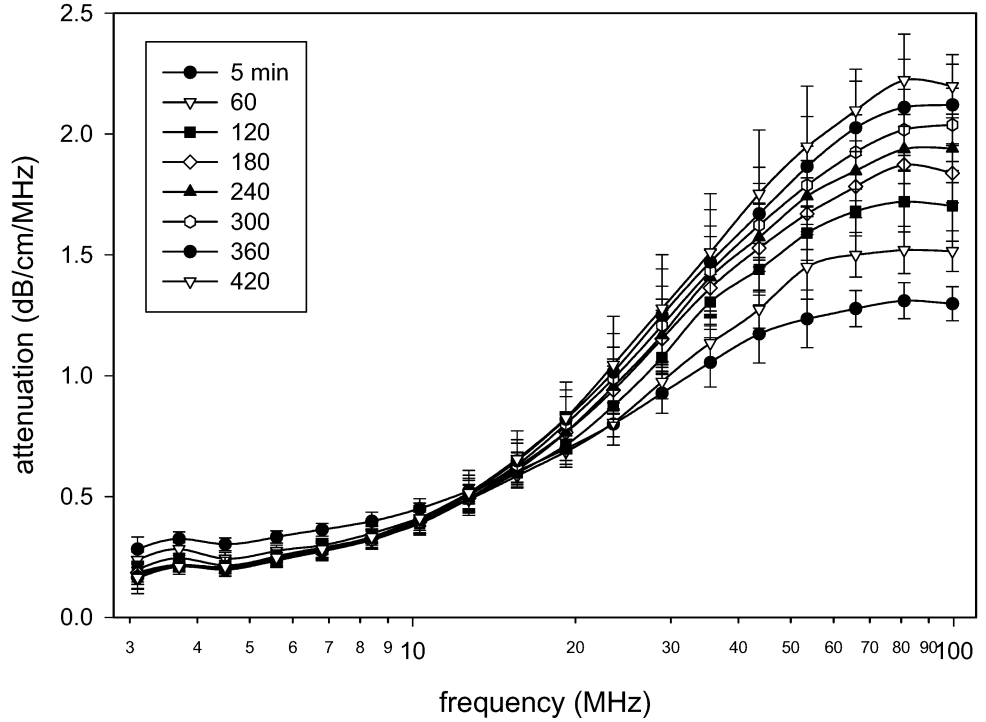

Fig. 8 Evolution of attenuation spectra for 2 % volume fraction CCRL 133 at different hydration times. Mean attenuation of 4 replicate experiments; vertical bars are standard deviations of replicates.

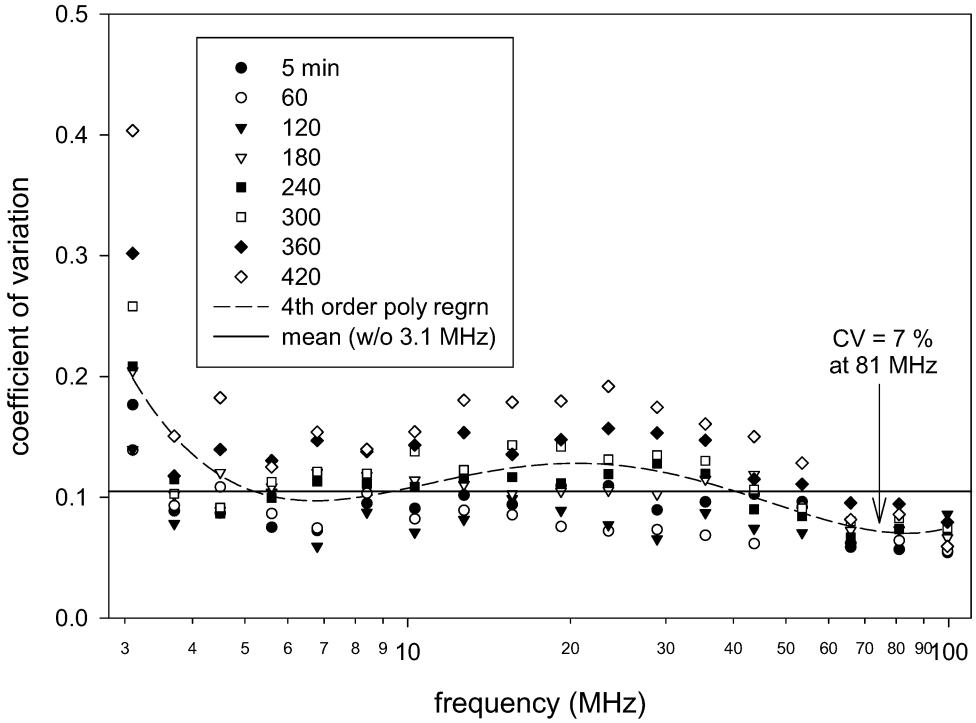

Fig. 9 Coefficient of variation as a function of frequency for attenuation data representing run-to-run repeatability of CCRL 133 at 2 % volume fraction. Data represents 4 replicate experiments.

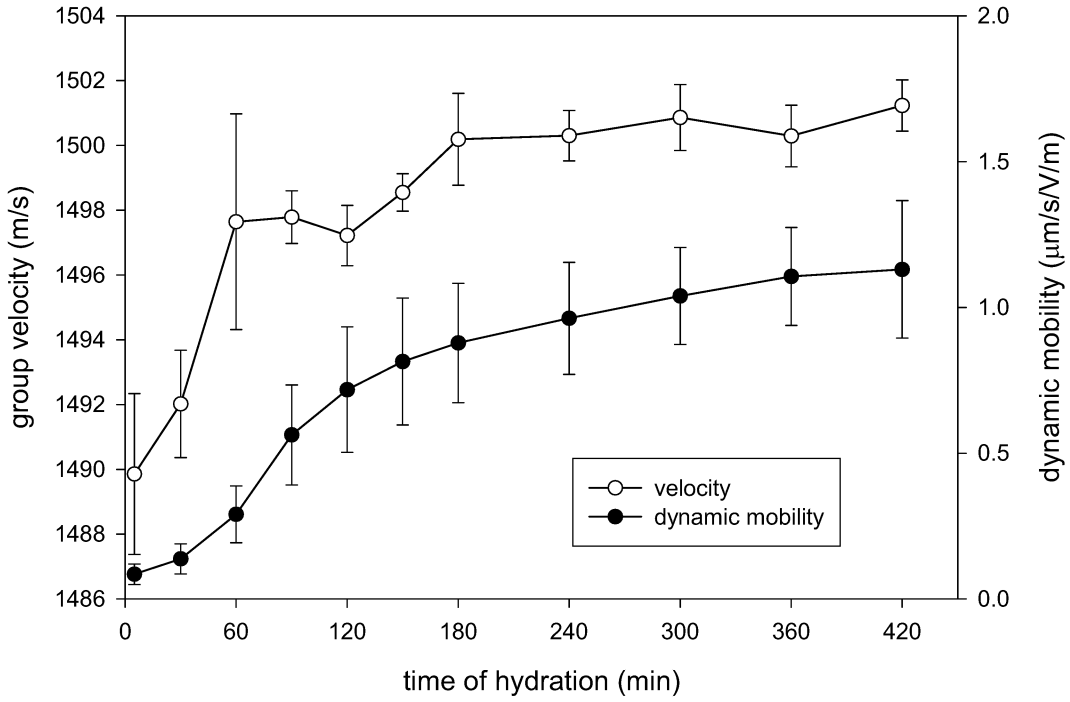

Fig. 10. Change in sound speed and electroacoustic response for 2 % volume fraction CCRL 133 as a function of hydration time. Mean and standard deviation of 4 replicate experiments.

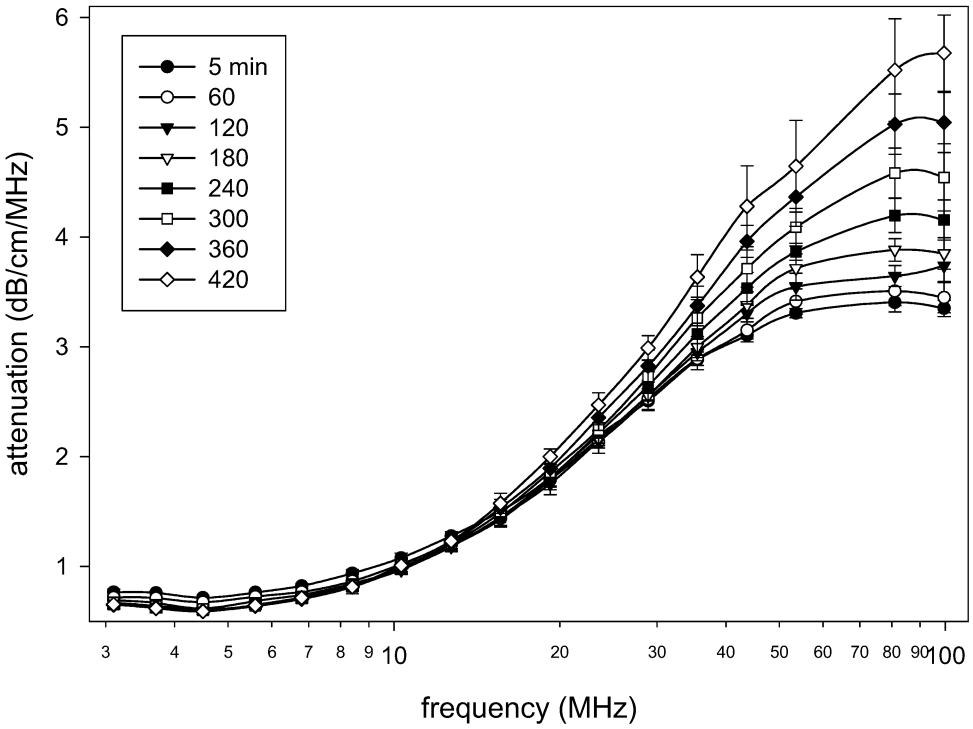

Fig. 11 Evolution of attenuation spectra for 5 % volume fraction CCRL 133 at different hydration times. Mean attenuation of 4 replicate experiments (2 replicates for 420 min); vertical bars show standard deviations.

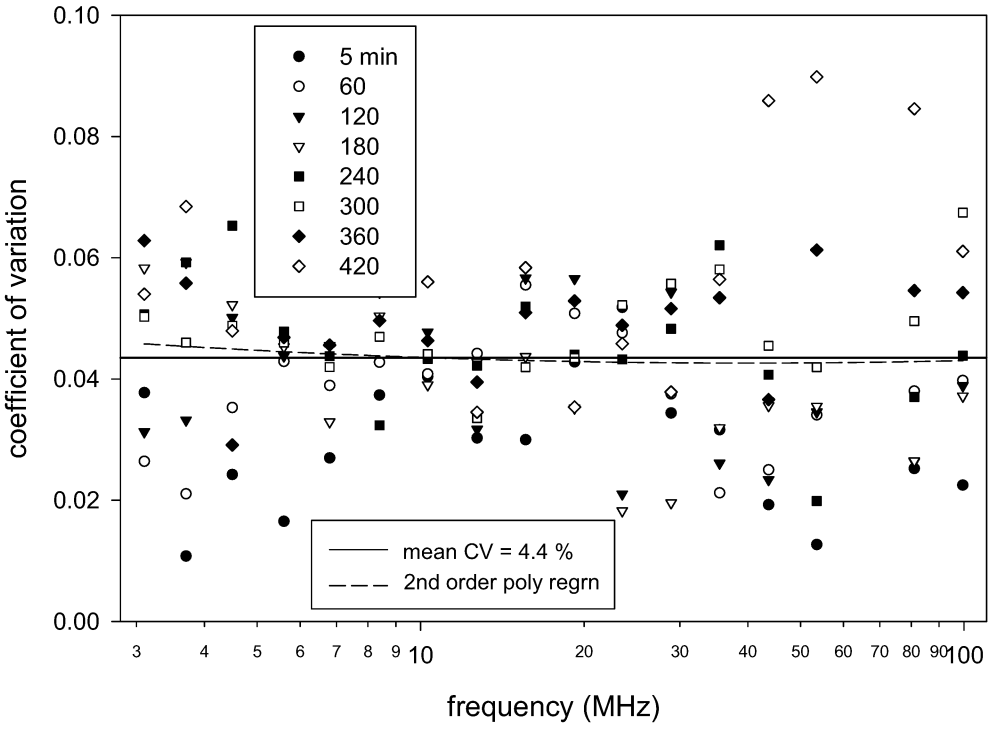

Fig. 12. Coefficient of variation as a function of frequency for attenuation data representing run-to-run reproducibility of CCRL 133 at 5 % volume fraction. Data represents 4 replicate experiments (2 replicates for 420 min).

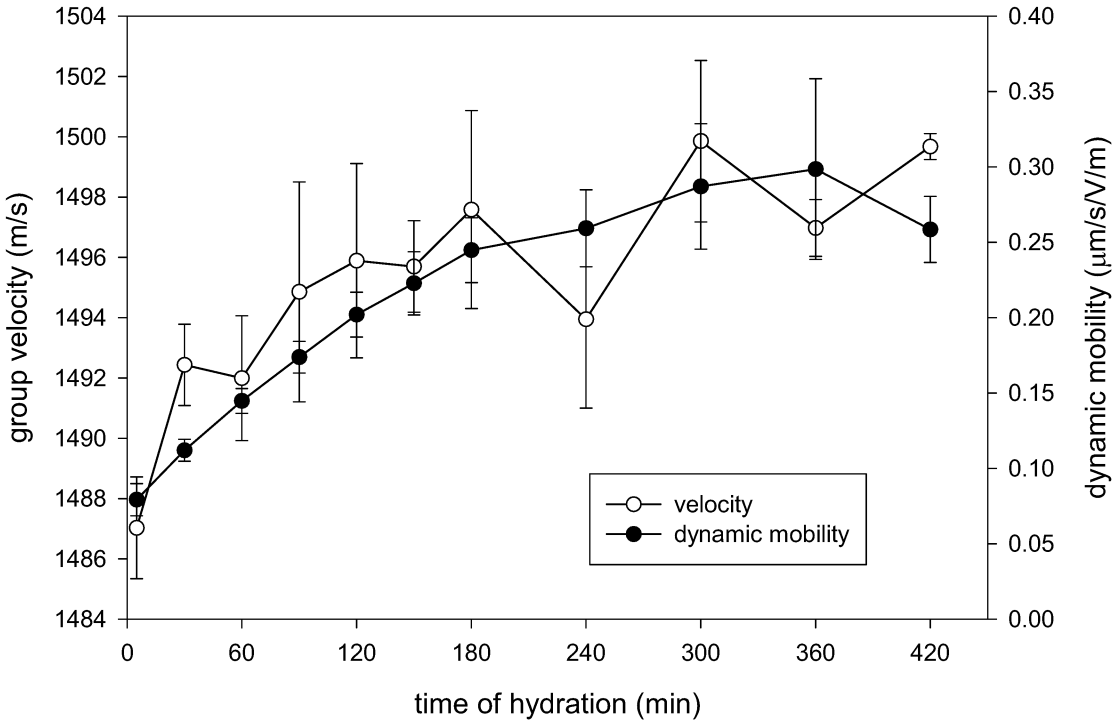

Fig. 13. Change in sound speed and electroacoustic response for 5 % volume fraction CCRL 133 as a function of hydration time. Mean and standard deviation of 4 replicate experiments (only 2 replicates for 420 min).

of aluminum oxide powders, one can expect CVs for repeatability of about 1 % over most of the frequency range for moderately concentrated suspensions. Repeatability decreases at high solids loadings (above 10 % volume fraction). Finally, Figure 10 shows the progressive change in group velocity and dynamic mobility with hydration time.

Figure 11 shows the attenuation spectra for 5 % volume fraction CCRL 133 as a function of hydration time for 4 replicate experiments under identical conditions performed on different days. Evolution is similar to 2 % data except for the relative magnitude. Figure 12 indicates an improvement in the CV values (typically 2 % to 6 %) relative to 2 % volume fraction. The frequency dependence is also more random and a dependence on hydration time is not obvious. Figure 13 shows the change in acoustic velocity and dynamic mobility with hydration time for 5 % volume fraction CCRL 133.

Figure 14 shows the attenuation spectra at different hydration times for 7.5 % volume fraction CCRL 133. Data represents the mean attenuation measured in 4 replicate experiments. Clearly, as the solids loading increases, the reproducibility improves but the sensitivity to changes caused by hydration is reduced. Figure 15 shows the change in group velocity and dynamic mobility over time. The magnitude of the dynamic mobility, and thus the underlying electroacoustic response, decreases as the solids loading increases. Figure 16 shows the CVs for replicate experiments. The CV values generally lie in the (2 to 8) % range, with a very slight dependence on frequency and hydration time.

Figure 17 shows the attenuation spectra measured for 15 % volume fraction CCRL 133 as a function of hydration time. Unlike previous data obtained at lower solids loadings, the spectra here show an increase with hydration time over the entire frequency range. The greatest sensitivity still occurs at the higher frequencies.

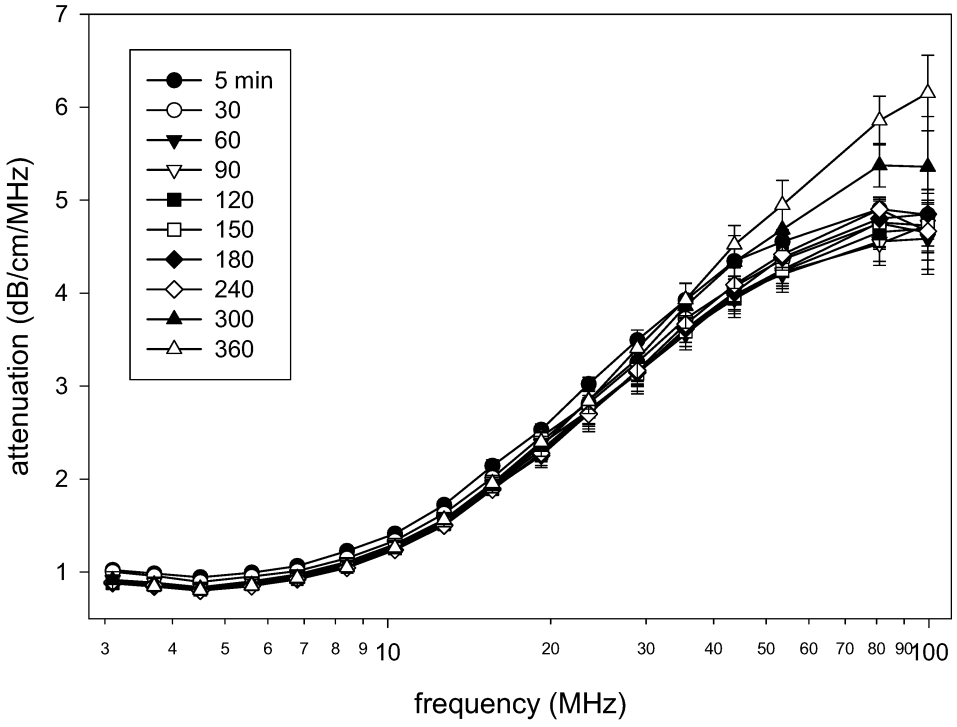

Fig. 14 Evolution of attenuation spectra for 7.5 % volume fraction CCRL 133 at different hydration times. Mean attenuation of 4 replicate experiments; vertical bars show standard deviations.

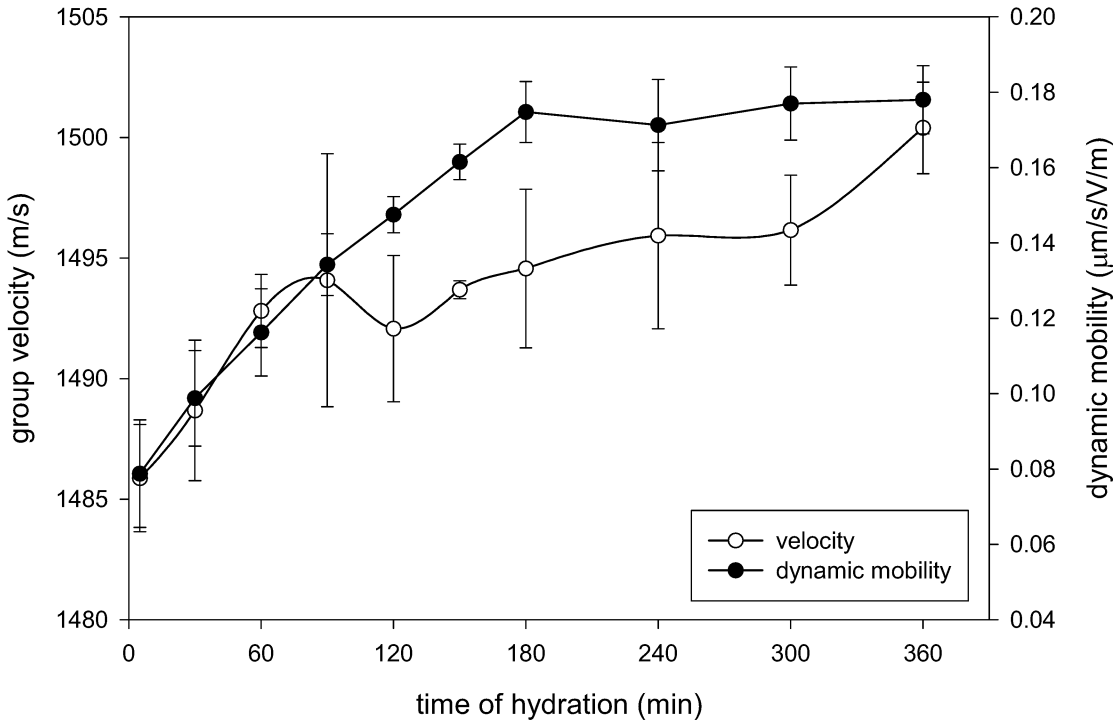

Fig. 15 Change in sound speed and electroacoustic response for 7.5 % volume fraction CCRL 133 as a function of hydration time. Mean and standard deviation of 4 replicate experiments.

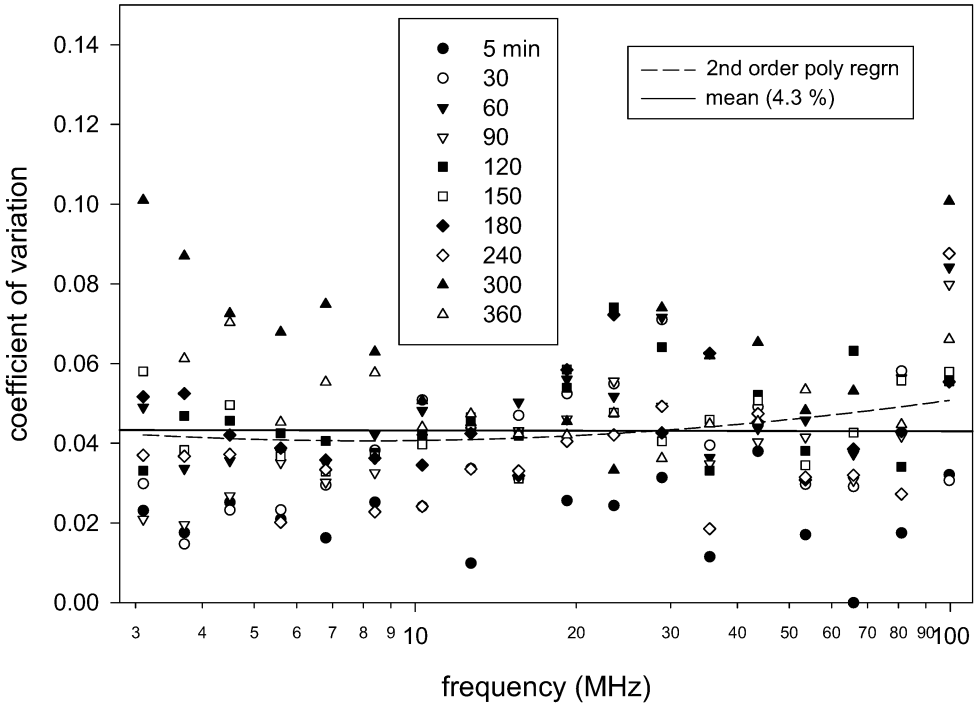

Fig. 16 Frequency distribution of coefficient of variation for attenuation data representing run-to-run reproducibility of CCRL 133 at 7.5 % volume fraction. Data represents 4 replicate experiments.

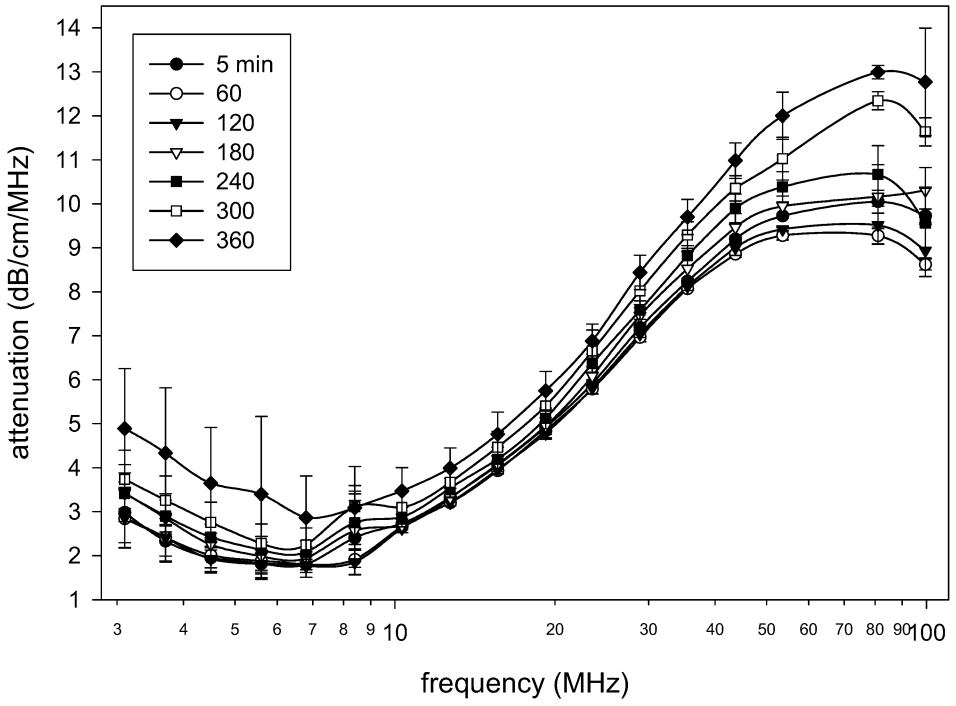

Fig. 17 Evolution of attenuation spectra for 15 % volume fraction CCRL 133 at different hydration times. Mean attenuation of 3 replicate experiments; vertical bars show standard deviations.

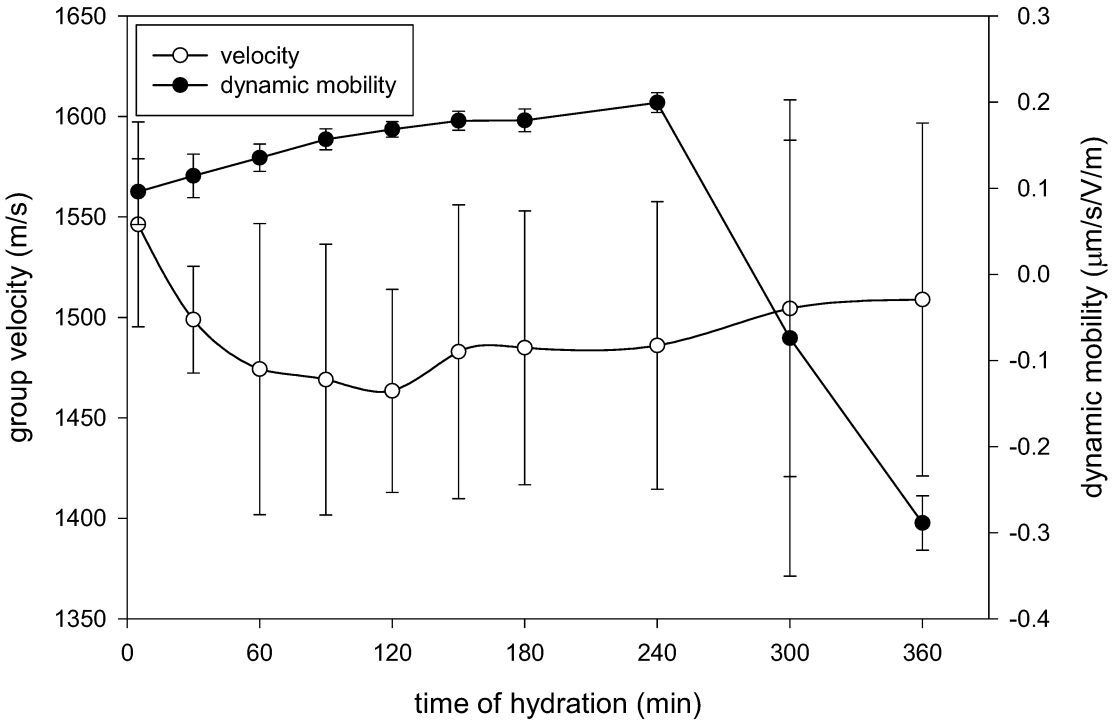

Fig. 18 Change in sound speed and electroacoustic response for 15 % volume fraction CCRL 133 as a function of hydration time. Mean and standard deviation of 3 replicate experiments.

Figure 18 shows the group velocity and dynamic mobility change with time for 15 % volume fraction CCRL 133. Again, in contrast to previous data at lower solids loadings, the velocity initially decreases with time and approaches a steady state. The dynamic mobility data is of questionable relevance due to the loss in sensitivity with increase in solids loading. An apparent switch in polarity is observed. All previous data for lower solids loadings indicate a net positive polarity.

Figure 19 shows the CVs for 15 % volume fraction CCRL 133. The magnitude of the CV range from a few % to about 25 % and is highly dependent on frequency. The data also indicates a moderate dependence on hydration time at some frequencies. The high frequency data above about 10 MHz is the most stable with respect to hydration time and the lowest with respect to overall magnitude.

Figure 20 shows the attenuation spectra for 20 % volume fraction CCRL 133. This is the highest solids loading evaluated in this study. The high frequency data exhibits a systematic increase in magnitude with hydration time, but the lower frequencies are fairly stable over time. One exception to this is data taken near 100 MHz (the upper limit of the frequency range), which is extremely noisy and unstable. Only a single complete experiment was performed for 20 % volume fraction, so an analysis of reproducibility is not provided.

Figure 21 gives the change in group velocity and dynamic mobility with hydration time for 20 % volume fraction CCRL 133. The data indicates a lack of sensitivity for electroacoustic measurements, but shows a fairly consistent and decreasing trend in mobility up to 5 h. The magnitude of the mobility is extremely low, however, and one cannot exclude contributions from dissolved ions in this case. Velocity measurements, on the other hand, suggest the presence of entrapped air bubbles or poor contact with the transducers, an issue that requires closer scrutiny.

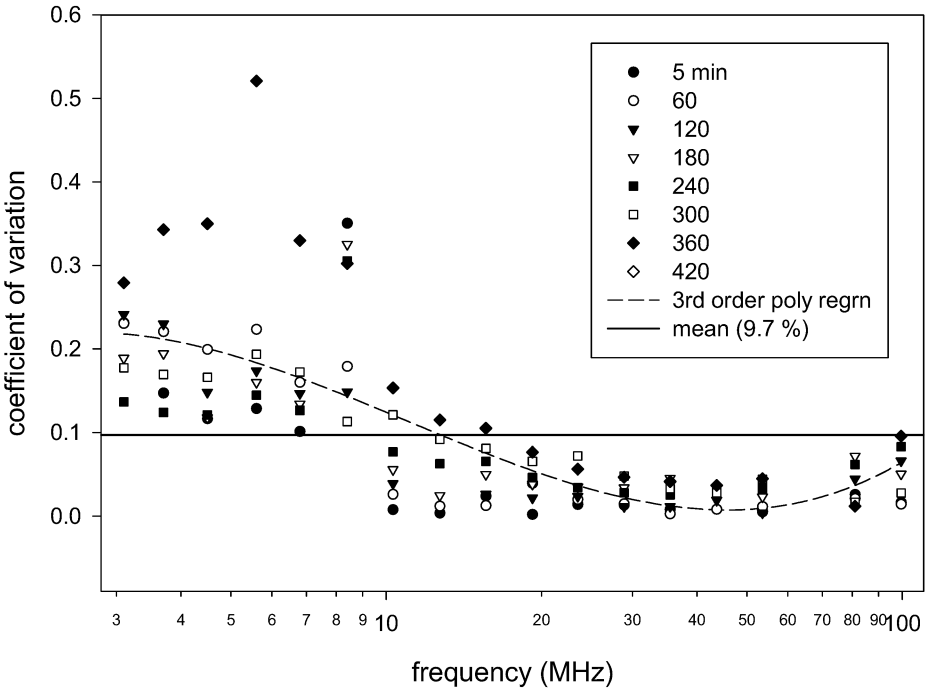

Fig. 19 Frequency distribution of coefficient of variation for attenuation data representing run-to-run repeatability of CCRL 133 at 15 % volume fraction. Data represents 3 replicate experiments.

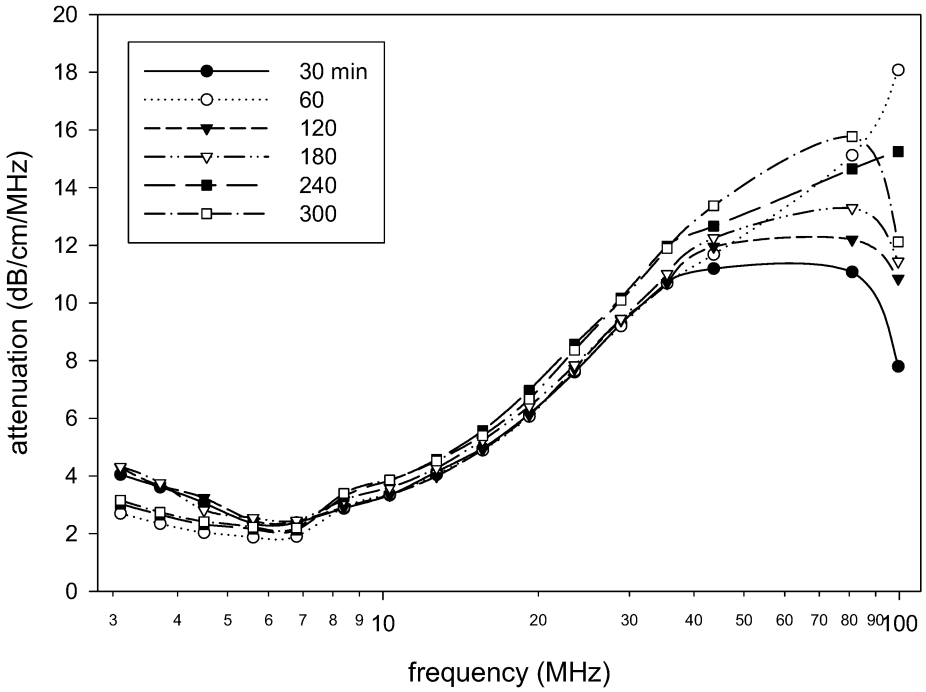

Fig. 20 Evolution of attenuation spectra for 20 % volume fraction CCRL 133 at different hydration times. Single experiment results.

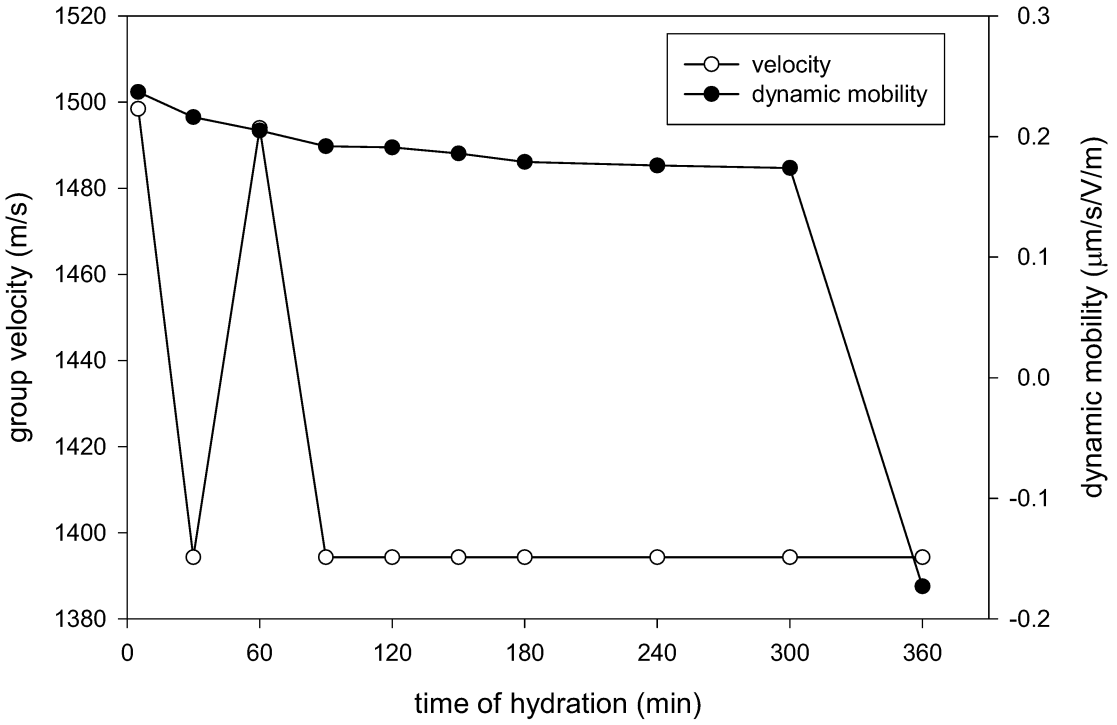

Fig. 21 Change in sound speed and electroacoustic response for 20 % volume fraction CCRL 133 as a function of hydration time. Single experiment results.

Solid phase volume fractions above 20 % were deemed too difficult to measure using the present experimental set up. Primary issues include the difficulty in pumping suspensions at high solids loadings, particularly in the latter stages of hydration, and the loss of sensitivity to changes occurring during hydration, at least in the tested frequency range. Alternative instrument designs and a broader frequency range may enable one to work with higher solid loadings, but were beyond the scope of the present work. The alkaline environment that cement presents should also not be discounted. This, coupled with the abrasive nature of the particles, can have a deleterious affect on the instrumentation. In particular, the moving transducer uses a gasket to seal the back end part from the test suspension. Problems have been encountered during this work that required adjustments to the gasket, removal and cleaning of the transducer, and use of different lubricating fluids to enable ease of motion without impacting the test materials. Further work may be required to optimize these issues for cement analysis.

Figures 22 and 23 show the dependence of acoustic attenuation on the solid phase volume fraction of CCRL 133, at a hydration time of 2 h, for the entire frequency range and for selected frequencies, respectively. In Figure 23, we find a reasonably good linear relationship between attenuation and volume fraction over a range of frequencies. The linear correlation improves if data for 20 % is excluded. Figures 24-26 show regression analysis of data at three select frequencies: 81 MHz, 28.9 MHz, and 15.6 MHz. A second order polynomial fit consistently provides an excellent fit to all data up to and including 20 %. This indicates that attenuation could potentially be used to determine the solid phase concentration in portland cement slurries, though the dependence on other factors would have to be examined more closely.

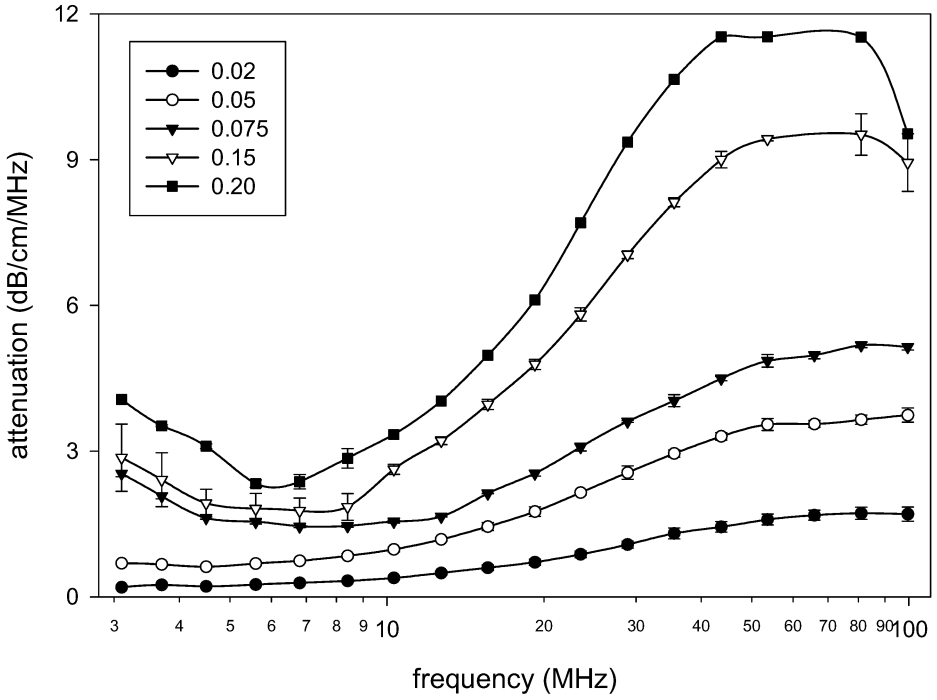

Fig. 22 Acoustic spectra for CCRL 133 at different solid phase volume fractions (see legend) and a hydration time t = 2 h. Mean and standard deviation of replicate measurements, except volume fraction 0.20 which represents a single experiment.

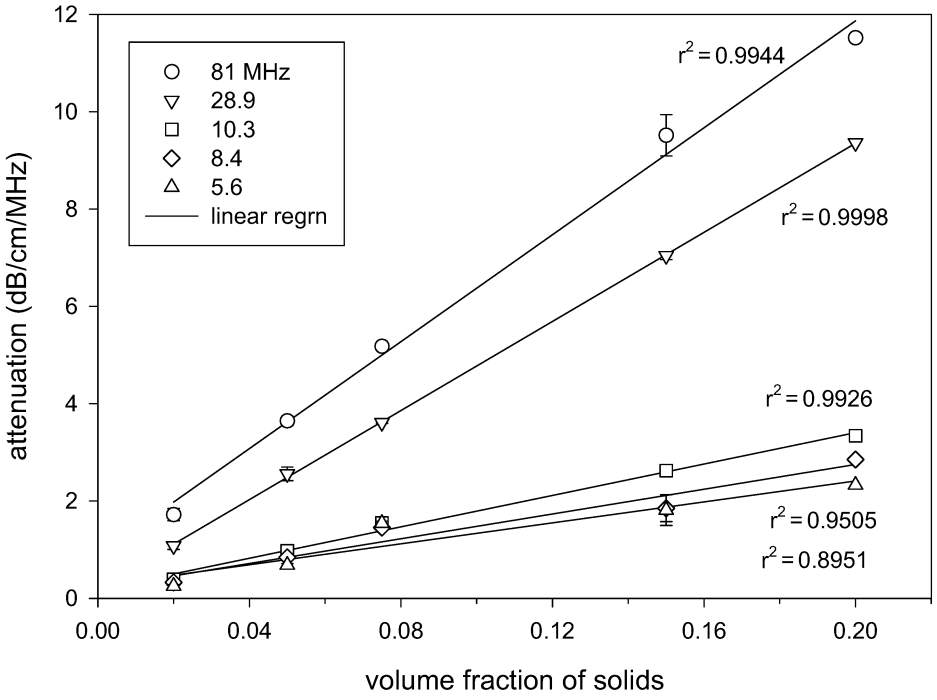

Fig. 23 Attenuation at different frequencies as a function of CCRL 133 volume fraction, and a hydration time of t = 2 h. Linear regression fits are shown.

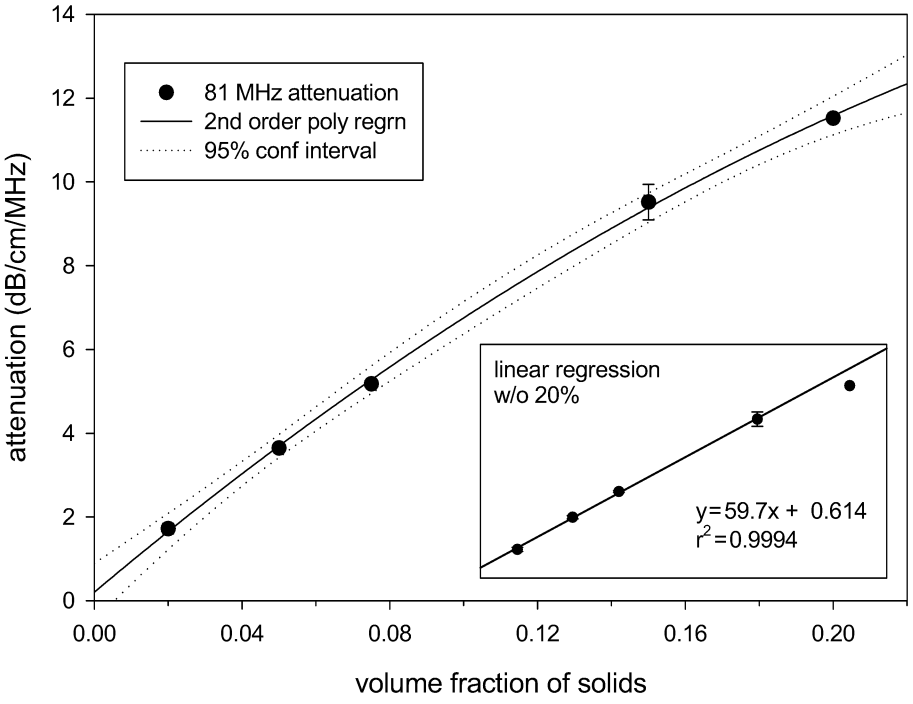

Fig. 24 Attenuation at 81 MHz and t = 2 h as a function of CCRL 133 volume fraction. Inset shows linear regression fit with data for 20 % not included.

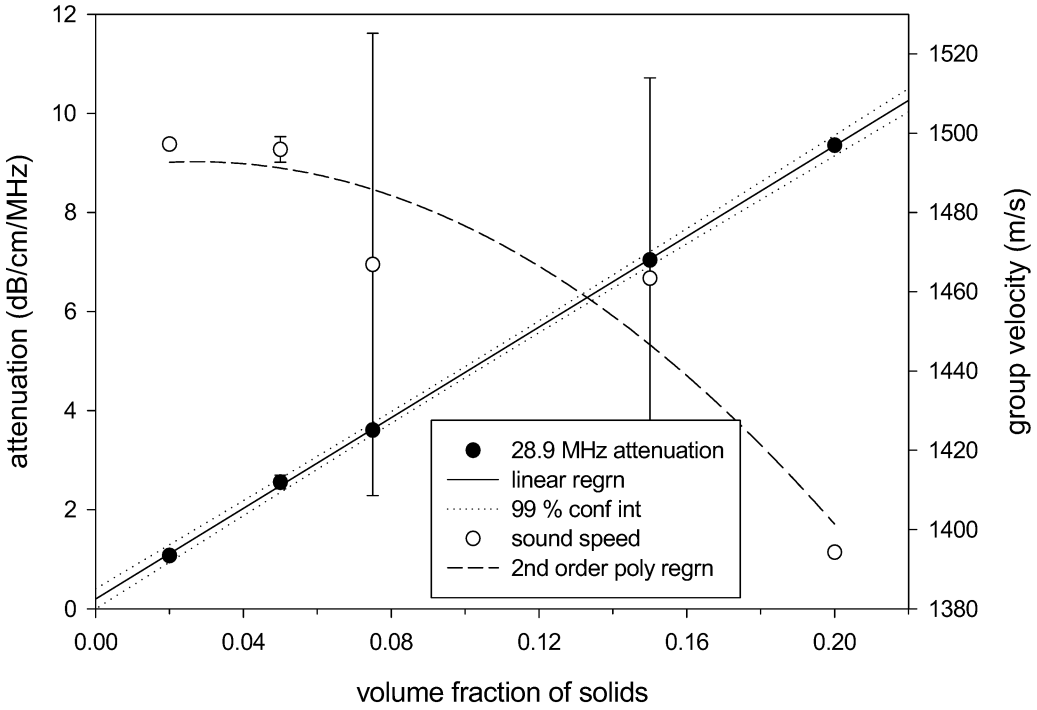

Fig. 25 Attenuation at 28.9 MHz and t = 2 h as a function of CCRL 133 volume fraction. Sound speed is also shown for comparison

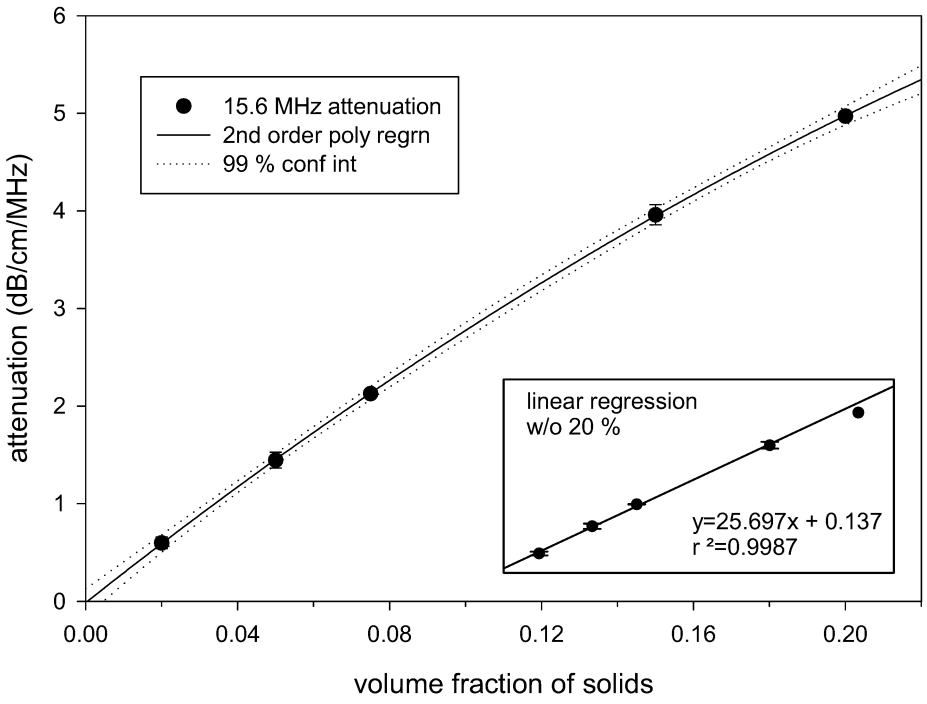

Fig. 26 Attenuation at 15.6 MHz and t = 2 h as a function of CCRL 133 volume fraction. Inset shows linear regression fit with data for 20 % not included.

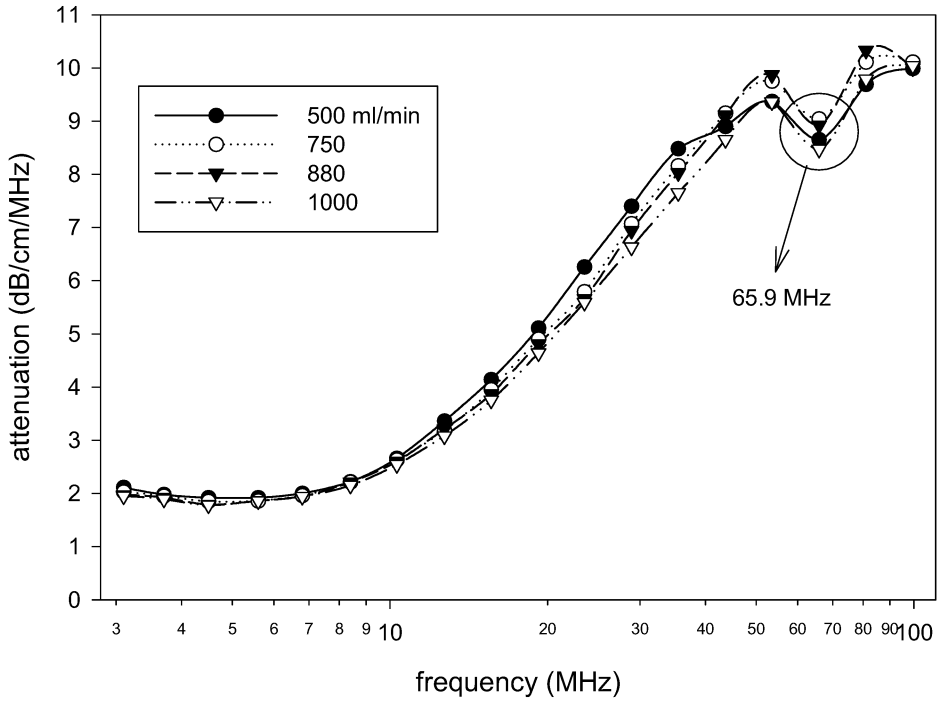

Fig. 27. Effect of peristaltic flow rate on the measured attenuation spectra for 15 % volume fraction CCRL 133 at t = 2 h. Minimum at 65.9 MHz is an artifact that manifests at higher solids loading.

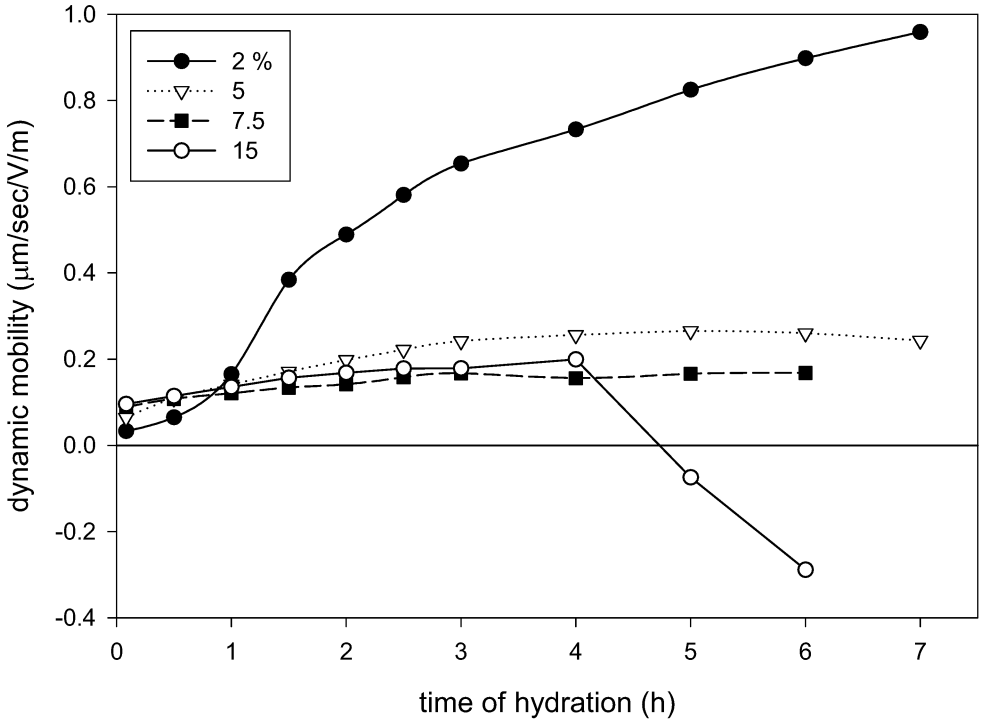

Fig. 28 Change in electroacoustic response with time at different solid phase volume fractions of CCRL 133.

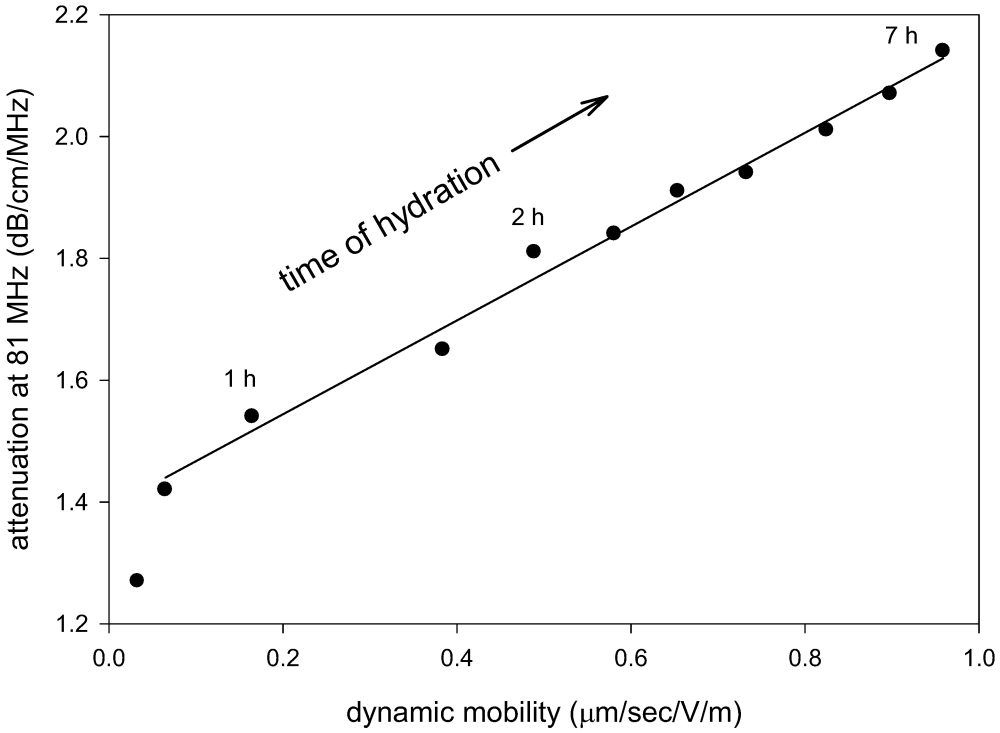

Fig. 29 Correlation between attenuation at 81 MHz and dynamic mobility for 2 % volume fraction CCRL 133 undergoing hydration.

Figure 27 examines the effect of the peristaltic flow rate on the measurement of attenuation spectra for 15 % volume fraction CCRL 133 at a hydration time of 2 h. There appears to be a slight dependence on flow rate at intermediate frequencies, but over the range (880 to 1000) ml/min, the differences are considered relatively small. The "dip" in attenuation observed at 65.9 MHz is an artifact related to the resonance frequency of the transducers and is only observed at the higher solid phase loadings.

Figures 28 and 29 summarize the electroacoustic results. Figure 28 shows the dynamic mobility versus hydration time for different solid phase loadings. Above 2 % volume fraction the sensitivity drops significantly, but at 2 % there is a strong correlation between mobility and attenuation after the initial 30 min. This is certainly a relationship worth exploring and had not, to the author's knowledge, been reported previously for cement.

Another interesting correlation is found between acoustic attenuation and the heat of hydration measured by differential thermal analysis (DTA). Figure 30 shows the DTA data used in the comparison (obtained from D. Bentz, NIST). In the data shown here, the heat of hydration was measured at a higher w/c ratio than was used in the acoustic measurements. The correlation in Figure 31 is strong and linear after the initial 3 h, which coincides fairly closely with the onset of the acceleration stage in cement hydration (see Figure 5).

This relationship deserves further attention and a more systematic study. It is interesting that attenuation appears to increase linearly from the earliest times measurable (pertaining to the initial hydrolysis and dormant periods), while the DTA data do not exhibit sensitivity to these early time changes. Attenuation spectroscopy may be a more sensitive probe for the initial formation of C-S-H precipitates.

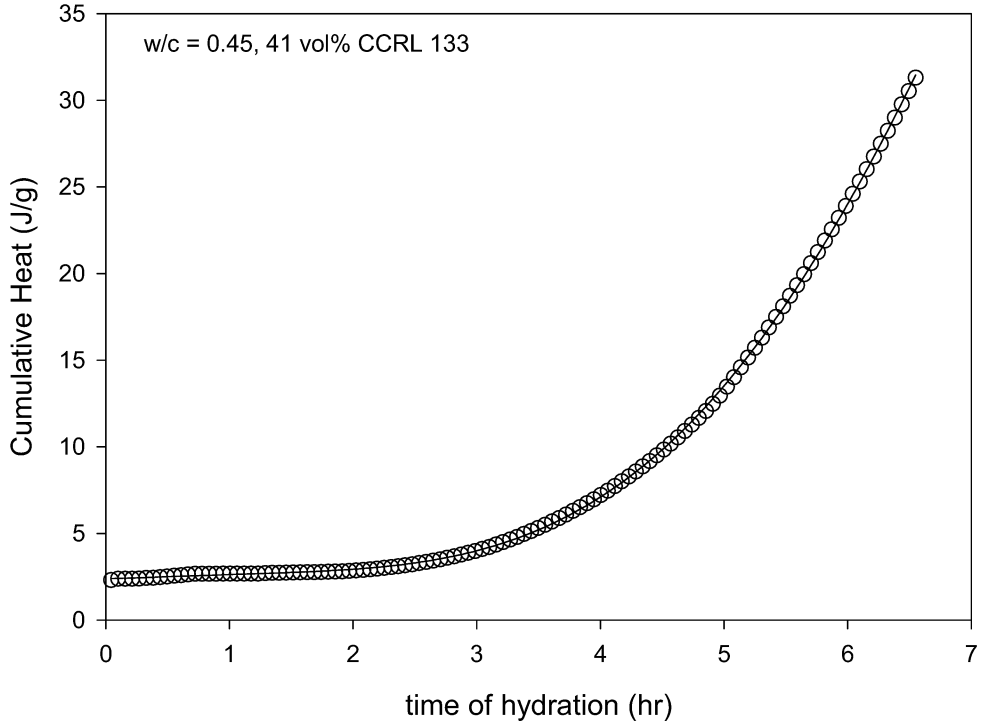

Fig. 30. Cumulative heat of hydration measured by differential thermal analysis (DTA) for CCRL 133 at w/c = 0.45. Data provided by Dale Bentz, NIST-BFRL.

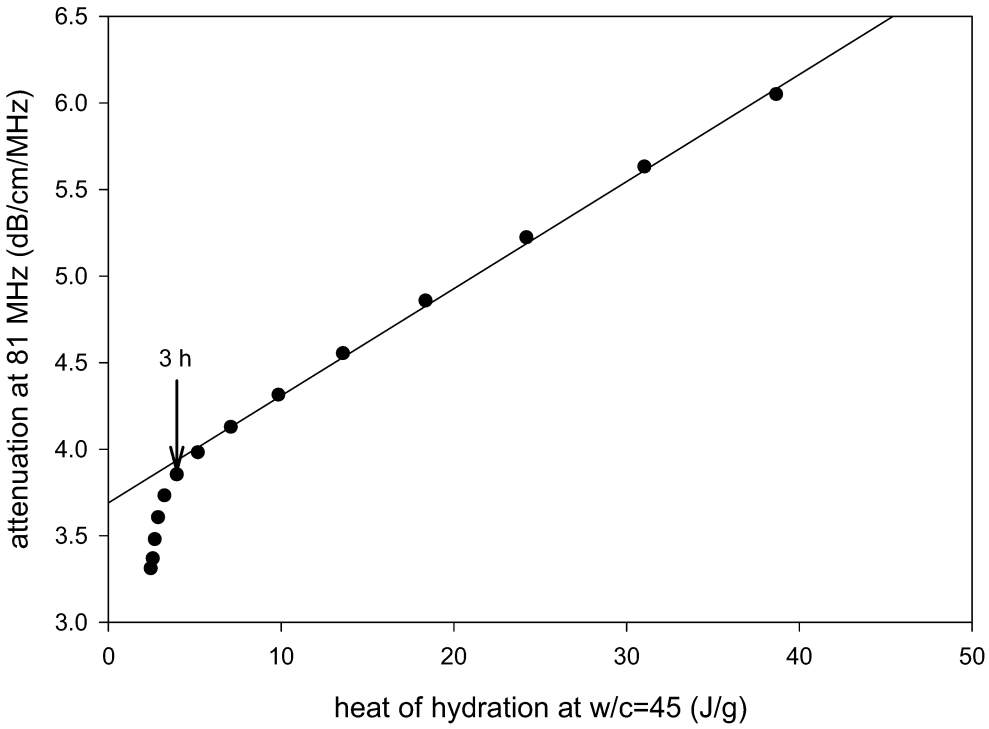

Fig. 31. Correlation between acoustic attenuation of hydrating CCRL 133 measured at 81 MHz for a 5 % volume fraction suspension and the cumulative heat of hydration determined for a paste with w/c = 0.45 or 41 % solid phase volume fraction.

Figure 32 demonstrates the ability of acoustic spectroscopy to assess the effect of HRWRAs, also known as superplasticizers or chemical admixtures, on the hydration of portland cement. Here the attenuation spectrum is plotted versus hydration time in the absence of additive on the left pane and with 1 % mass fraction (relative to the solid phase) naphthalene sulfonate on the right pane. The retardation effect is clear, as the spectra remain nearly unchanged for up to 6 h when HRWRA is present.

Figures 33 through 36 track the attenuation measured at two frequencies (81 MHz and 28.9 MHz) for a series of commercial HRWRA formulations (see also Table 1) at two different dosages (mass fraction relative to the solid phase). Data was obtained for suspensions containing 7.5 % volume fraction CCRL 133. As expected, the higher frequency appears to yield better sensitivity to the changes (or lack thereof) occurring during hydration. Attenuation at 81 MHz exhibits a greater relative change over time. The effect of HRWRA concentration is also consistent, with the 1 % addition producing a greater retardation relative to 0.2 % addition.

By contrast, acoustic velocity and dynamic mobility are much less sensitive to the presence of chemical admixtures, as demonstrated in Figures 37 and 38 for two HRWRA formulations. Furthermore, the trends are less clear compared with attenuation measurements. It is feasible that sensitivity with respect to electroacoustic measurements can be improved by going to lower solid phase volume fractions, and this may be worth examining in more detail.

But clearly, attenuation spectra are a sensitive measure of the retardation due to HRWRA addition, and attenuation spectroscopy shows great promise for quantifying and monitoring the effects of HRWRAs during the early hydration period.

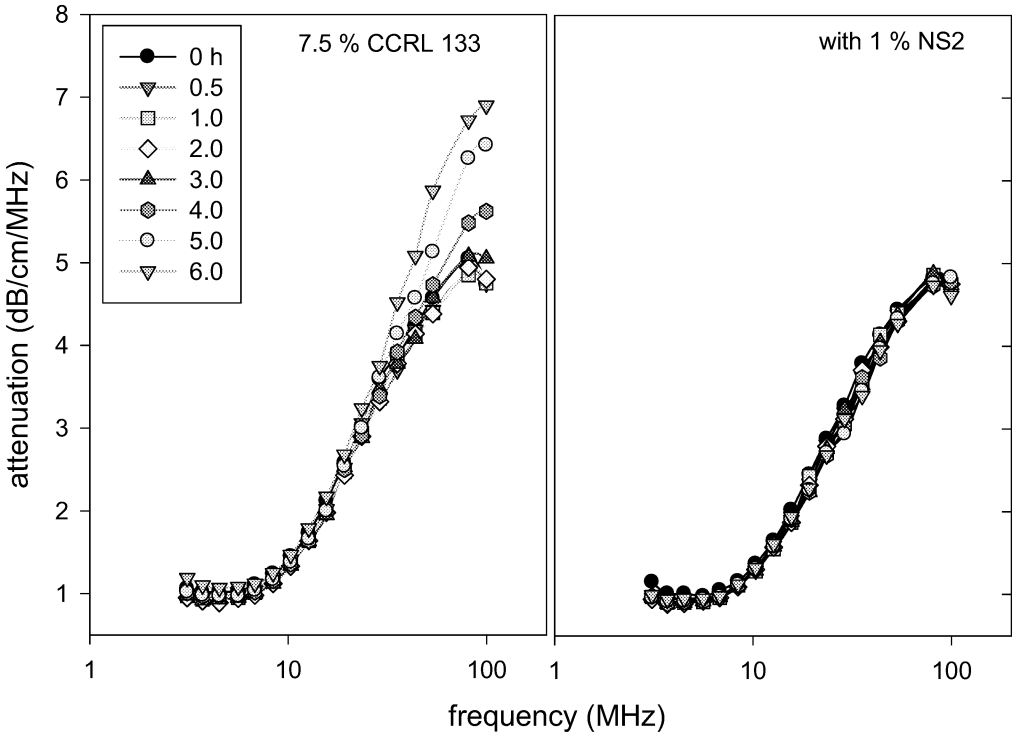

Fig. 32. Effect of the addition of chemical admixture (1 % by mass naphthalene sulfonate) on hydration of 7.5 % volume fraction CCRL 133 as indicated by acoustic attenuation spectra measured at different hydration times.

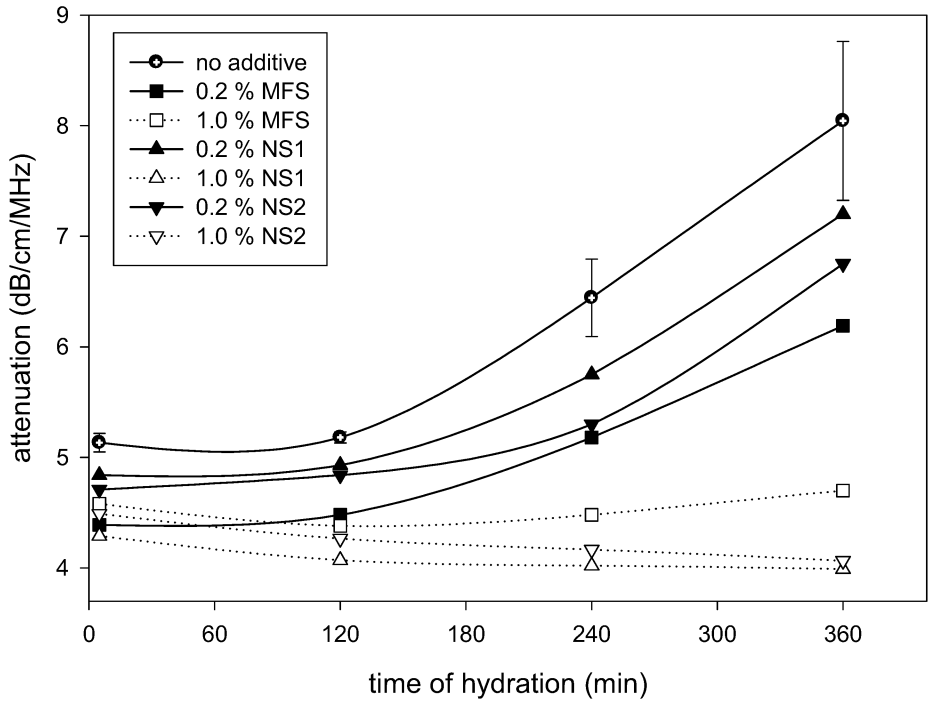

Fig. 33. Attenuation at 81MHz for 7.5 % volume fraction CCRL 133 showing the effect of chemical admixtures at two mass fraction dosages relative to the solid phase: two naphthalene sulfonates and a melamine formaldehyde sulfonate formulation.

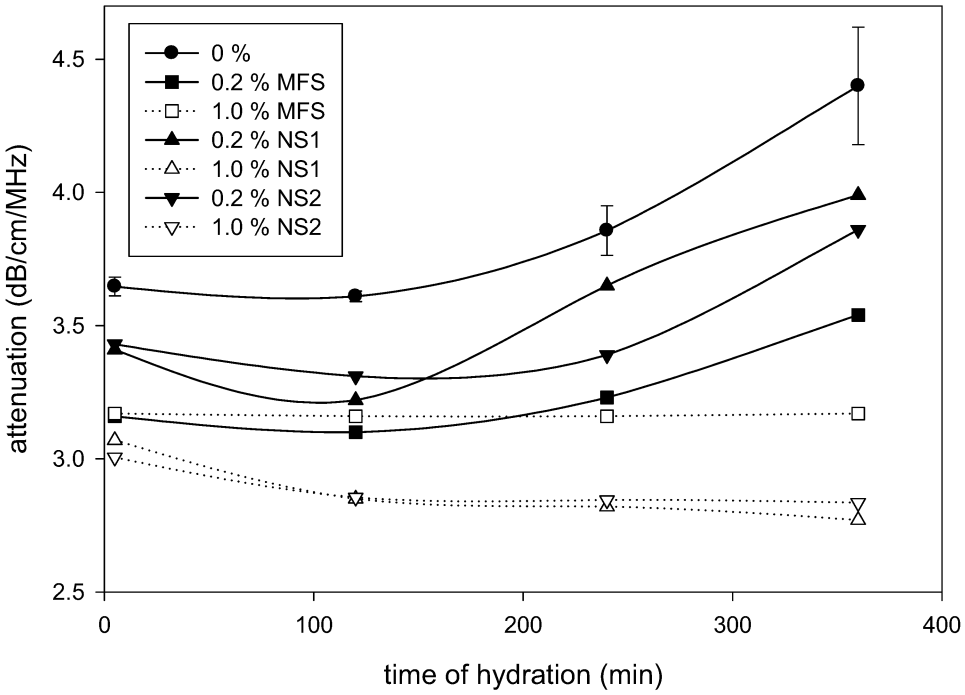

Fig. 34. Attenuation measured at 28.9 MHz for 7.5 % volume fraction CCRL 133 showing the effect of chemical admixtures at two mass fraction dosages relative to the solid phase: two naphthalene sulfonates and a melamine formaldehyde sulfonate formulation.

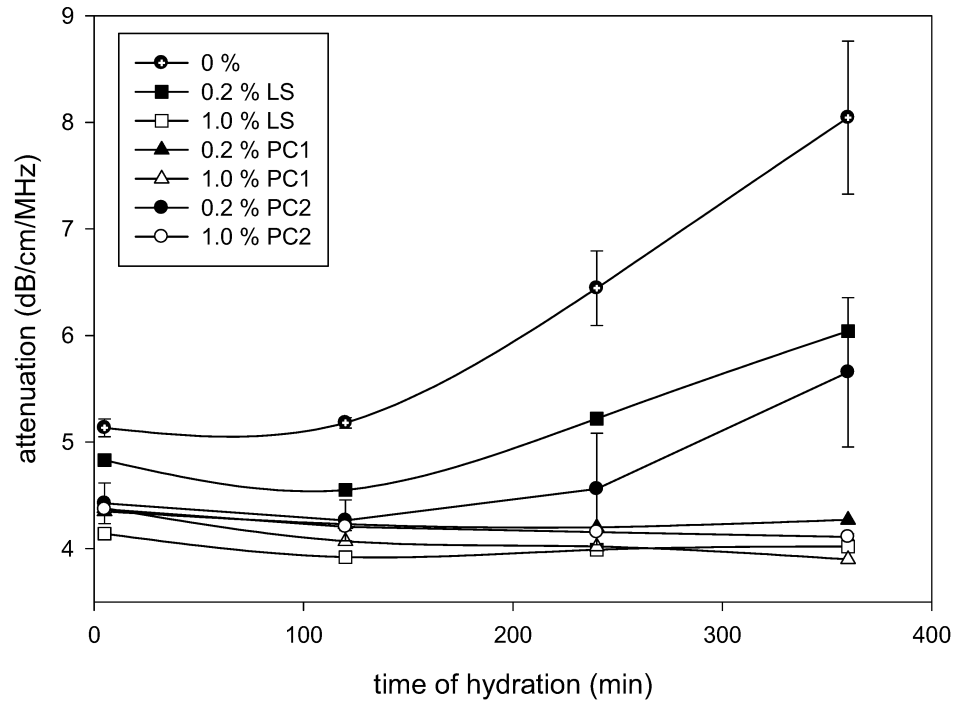

Fig. 35. Attenuation measured at 81MHz for 7.5 % volume fraction CCRL 133 showing the effect of chemical admixtures at two mass fraction dosages relative to the solid phase: a lignosulfonate and two polycarboxylate formulations.

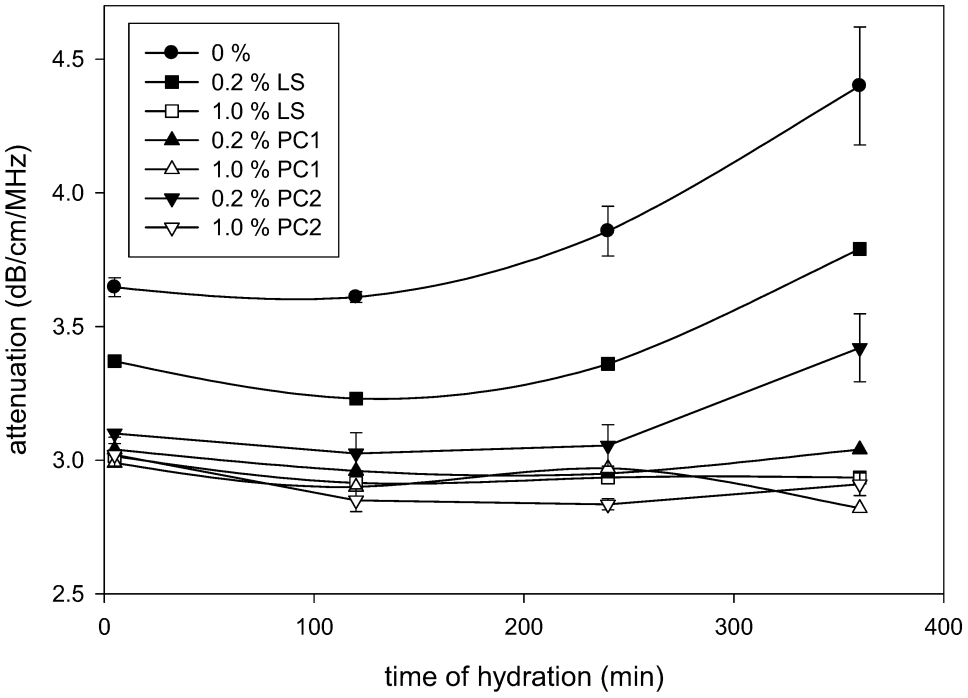

Fig. 36. Attenuation measured at 28.9 MHz for 7.5 % volume fraction CCRL 133 showing the effect of chemical admixtures at two mass fraction dosages relative to the solid phase: a lignosulfonate and two polycarboxylate formulations.

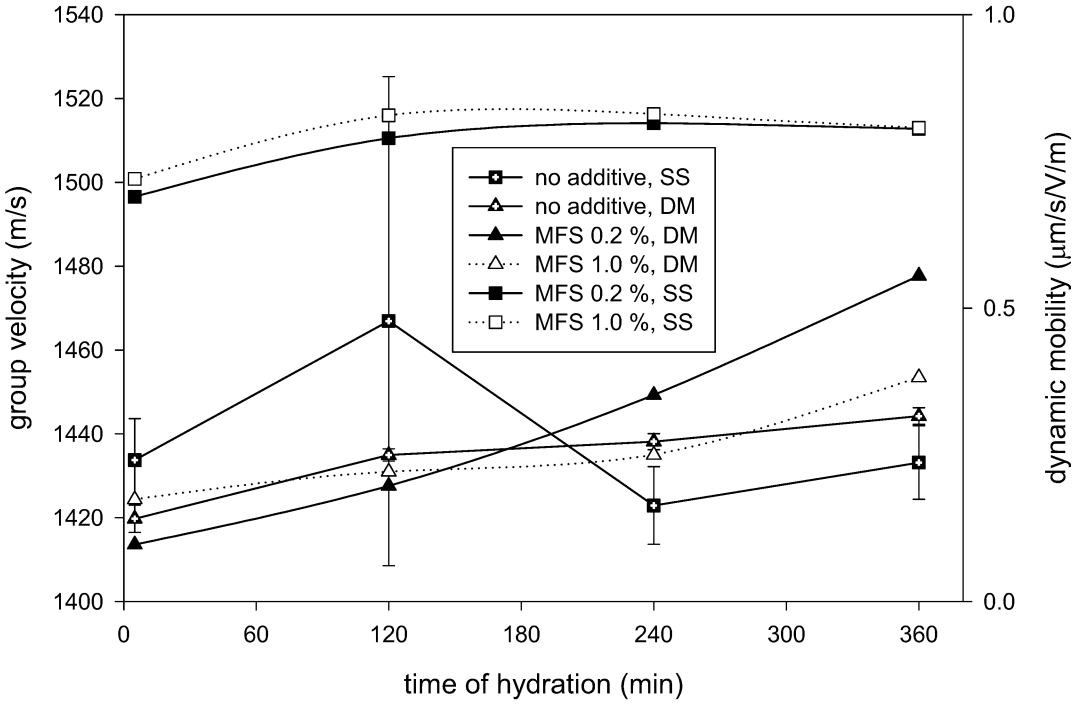

Fig. 37. Group velocity and dynamic mobility for 7.5 % volume fraction CCRL 133 showing the effect of chemical admixture melamine formaldehyde sulfonate at two mass fraction dosages relative to the solid phase.

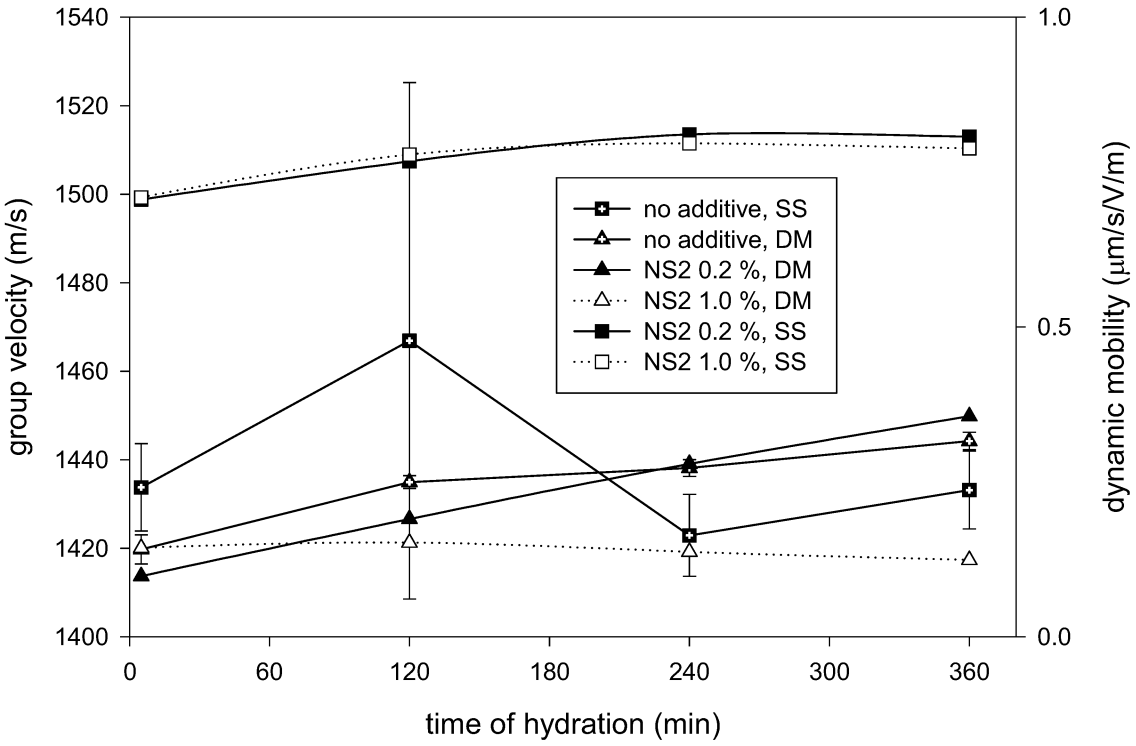

Fig. 38. Group velocity and dynamic mobility for 7.5 % volume fraction CCRL 133 showing the effect of chemical admixture naphthalene sulfonate at two mass fraction dosages relative to the solid phase.

5. Conclusions

MHz-frequency acoustic spectroscopy has been demonstrated to show promise as an effective technique for in situ characterization, monitoring, and possibly quantification of early hydration in portland cement suspensions. It is believed that the observed sensitivity is linked to precipitation and growth of the nanoscale C-S-H phase. The high frequency portion of the acoustic spectrum is more sensitive to its presence and less affected by the coarser components of the clinker.

Based on the experience gained during the course of this exploratory study, and on data and observations resulting from that effort, we offer the following conclusions and suggestions for future work.

For solid volume fractions below 7.5 %, attenuation is constant near 16 MHz, independent of hydration time. Additionally, attenuation below about 30 MHz scales linearly with solids loading up to at least 20 % volume fraction. This suggests that lower frequency data may be appropriate for determining solids concentration, though it is not immediately clear if this would be beneficial from a practical standpoint. Acoustic theory predicts that larger size particulate components (in the micrometer range) will scatter strongly at lower frequencies. Attenuation for smaller submicrometer particles is dominated by viscous loss occurring at higher frequencies. So the attenuation observed in CCRL 133 at low frequencies may be due primarily to the clinker phase, which would explain why it does not evolve with time in such relatively dilute suspensions. From 7.5 % upwards, attenuation is only mildly dependent on time in the low frequency range (the exception is 15 %, which may be an anomaly or may indicate some other issue yet unidentified).

Additionally, the lack of sensitivity at lower frequencies suggests that measurements

intended to follow hydration could be restricted to one or a few selected frequencies, thus speeding up the analysis time and providing better time resolution.

We also observe that as the solids loading increases, sensitivity to changes in the electroacoustic response decrease. The CVI measurements, performed in parallel with acoustic attenuation measurements, are useful only at solids concentrations below about 5 % in portland cement. Additionally, known interference from solution phase ionic species must be addressed in a more quantitative analysis of data. This was beyond the scope of the present exploratory work. Without taking into consideration the ionic contributions to the signal, systematic errors will be significant and will adversely impact any interpretation of results. The usefulness of electroacoustic measurements for analysis of hydrating portland cement is thus limited.

Acoustic velocity (sound speed) measurements, though simple and fast, do not appear to offer sufficient sensitivity to changes during early hydration in comparison to attenuation measurements. On the other hand, for quantitative size analysis using acoustic spectroscopy, sound speed measurements are necessary. Size analysis is probably not feasible in the case of portland cement suspensions, due to the complexity of components and wide range of sizes present.

The “dip” in attenuation observed in some spectra at 65.9 MHz, especially at higher solid loadings, is due to this being a “blind spot” for the transducer. It is close to double the resonance frequency near 35 MHz. At the resonances frequency the transducer efficiency is highest, and decreases below this value. At even multiples (e.g., 2×, 4×) there are blind spots where the efficiency drops to very low values. Thus as the solids concentration increases, attenuation increases and the low signal at 65.9 MHz is reduced further, causing a negative measurement error and resulting in the observed dip in the spectrum. This data point can, and should, be ignored, and the software can be programmed to exclude points with negative error.

One of the interesting results to come out of this study is the apparent close correlation between attenuation at high frequencies and the heat of hydration determined by DTA. This relationship needs to be explored more systematically, and in particular using w/c ratios that overlap for both techniques in order to avoid possible differences due to the solid phase concentration. Based on the limited data available, we speculate that acoustic spectroscopy may exhibit greater sensitivity relative to DTA for the very early stages of hydration (before about 3 h).

Perhaps the most intriguing results relate to the ability of high frequency acoustic attenuation to characterize the retardation produced by chemical admixtures. This promises to be a fruitful area for future research, as it provides a rapid method for quantifying and comparing the retardation effect during early hydration for different formulations of additives. Acoustic sensing may save time and expense associated with more traditional and time consuming approaches for screening of chemical admixture formulations.

To better refine the methodology and improve the current understanding of the underlying attenuation processes in hydrating cement suspensions, it is suggested that future work focus on cleaner systems with fewer components. Pure C_3S phases or pre-classified narrow size distribution subsets of portland cement might be suitable for such studies. In that way, it may be possible to quantify the effect of various cement components on the frequency-dependent attenuation. This should be done in parallel with modeling efforts to predict acoustic loss based on component size, composition, and concentration.

Finally, as a corrosive and abrasive material, prolonged experiments involving cement have

proven to be a challenge with respect to their effects on sensor components. So, the development of a simple, robust fixed-frequency attenuation measurement device with no moving parts in contact with the cement suspension would be beneficial and probably necessary for routine testing applications.

Acknowledgements

Chemical admixtures were provided by W.R. Grace (Construction Products Division, Cambridge, MA) and Degussa Construction Chemicals (Master Builders Technology, Cleveland, OH). Dispersion Technology Inc. (Bedford Hills, NY) provided critical instrument support and responded to specific needs related to cement analysis. The Cement and Concrete Reference Laboratory (CCRL) supplied the test cement for these studies. Dale Bentz (NIST) provided the thermal data for CCRL 133.

Glossary

acoustic Having to do with sound waves and especially their production, transmission and interaction with matter.

acoustic attenuation Reduction in the intensity of sound (sound energy) propagating in a medium, via various loss mechanisms (e.g., thermal, viscous, scattering). Characterized by the attenuation coefficient, α, typically expressed as *decibels* (dB) per unit length and often normalized to the frequency.

acoustic impedance Complex ratio of sound pressure to the sound particle velocity within the medium through which sound propagates. Useful for characterizing the interaction of sound waves at a boundary between two phases.

compression wave A wave whose oscillations are parallel to the direction of propagation, and the motion of the propagating medium is in the same direction as the motion of the wave. These are also referred to as longitudinal or pressure waves.

decibel (dB) In acoustics, a dimensionless logarithmic measure of sound intensity. The decibel is equal to ten times the common logarithm of the ratio of the sound intensity of the source (e.g., a signal transmitted through a medium) relative to a reference sound intensity. The reference is commonly specified as a sound pressure level (SPL) relative to 1 μPa in non-gaseous media (ANSI S1.1-1994).

hertz (Hz) Frequency of sound expressed by cycles per second.

shear wave A wave whose oscillations are perpendicular to the direction of propagation (a transverse wave). Shear waves can only propagate in elastic solids, as they are rapidly dissipated in fluid media. Shear waves travel slower than compression waves.

sound intensity Average rate of sound energy transmitted in a specified direction at a point through a unit area normal to this direction at the point considered; in units of watts per square meter (W/m^2); symbol, I (ANSI S1.1-1994).

sound intensity level (SIL) Ten times the common logarithm of the ratio of the intensity of a given sound in a stated direction to the reference sound intensity of 1 picoWatt per square meter (pW/m^2); in units of decibels (dB) (ANSI S1.1-1994).

sound speed The speed of sound describes the velocity (typically in m/s) of sound waves propagating through a medium. Sound speed varies depending on the medium and with thermophysical properties of the medium, especially temperature and density. Sound speed is also frequency-dependent in dispersive media such as water. Should not be confused with *sound particle velocity*, which describes the velocity of the constituent "particles" of the medium as they move in response to a passing sound wave. In a homogenous fluid, the sound speed is equal to $\sqrt{K/\rho}$, where K is the adiabatic bulk modulus and ρ is the bulk density.

The speed of sound in pure water is 1497 m/s at 25 ºC.

ultrasonic Referring to sound frequencies above the normal human range of hearing (i.e., higher than about 20 KHz).

References

1. S. Mindess and J. F. Young, "Hydration of portland Cement," *Concrete,* (Prentice-Hall, Englewood Cliffs, N.J., 1981), 76-111.

2. P. D. Tennis and H. M. Jennings, "A model for two types of calcium silicate hydrate in the microstructure of portland cement pastes," *Cement and Concrete Research* **30**, 855-863 (2000).

3. J. J. Thomas, H. M. Jennings, and A. J. Allen, "The surface area of cement paste as measured by neutron scattering: Evidence for two C-S-H morphologies," *Cement and Concrete Research* **28**, 897-905 (1998).

4. D. P. Bentz, E. J. Garboczi, C. J. Haecker, and O. M. Jensen, "Effects of cement particle size distribution on performance properties of portland cement-based materials," *Cement and Concrete Research* **29**, 1663-1671 (1999).

5. M. R. Ismail and S. A. S. Elhemaly, "Hydration kinetics of cement paste containing concrete admixture," *Cement and Concrete Research* **21**, 683-690 (1991).

6. F. Puertas and T. Vazquez, "Early hydration cement. Effect of admixtures superplasticizers," *Materiales de Construccion* **51**, 53-61 (2001).

7. Uchikawa, H. Function of Organic Admixture Supporting High Performance Concrete. Cabrera, J. G. and Rivera-Villarreal, R. International Symposium on the Role of Admixtures in High Performance Concrete, 69-96. 1999. Bagneux, France, RILEM Publications. 3-21-1999.

8. A. Capmas, D. Menetrier-Sorrentino, and D. Damidot, "Effect of temperature on setting times of calcium aluminate cements," *Calcium Aluminate Cements,* R. J. Mangabhai, ed., (Chapman & Hall, London, 1990), 65-80.

9. S. P. Jiang, J. C. Mutin, and A. Nonat, "Studies on mechanism and physico-chemical parameters at the origin of the cement setting: I. The fundamental processes involved during the cement setting," *Cement and Concrete Research* **25**, 779-789 (1995).

10. M. Y. A. Mollah, F. Lu, R. Schennach, and D. L. Cocke, "An x-ray diffraction, Fourier-transform infrared spectroscopy, and scanning electron microscopy/energy- dispersive spectroscopic investigation of the effect of sodium lignosulfonate superplasticizer on the hydration of portland cement Type V," *Polymer-Plastics Technology and Engineering* **38**, 849-868 (1999).

11. E. E. Hekal, M. Abd-El-Khalek, G. M. El Shafey, and F. S. Hashem, "Mechanical and physico-chemical properties of hardened portland cement pastes containing hydrophobic admixtures - Part 1: Compressive strength and hydration kinetics," *Zkg International* **52**, 697-700 (1999).

12. S. Long, C. Liu, and Y. Wu, "ESCA study on the early C3S hydration in NaOH solution and pure water," *Cement and Concrete Research* **28**, 245-249 (1998).

13. S. K. Agarwal, I. Masood, and S. K. Malhotra, "Compatibility of superplasticizers with different cements," *Construction and Building Materials* **14**, 253-259 (2000).

14. J. I. Bhatty, "A Review of the application of thermal-analysis to cement admixture systems," *Thermochimica Acta* **189**, 313-350 (1991).

15. P. Gu and J. J. Beaudoin, "A conduction calorimetric study of early hydration of ordinary portland cement high alumina cement pastes," *Journal of Materials Science* **32**, 3875-3881 (1997).

16. V. S. Ramachandran and M. S. Lowery, "Conduction calorimetric investigation of the effect of retarders on the hydration of portland-cement," *Thermochimica Acta* **195**, 373-387 (1992).

17. M. A. Simard, P. C. Nkinamubanzi, C. Jolicoeur, D. Perraton, and P. C. Aitcin, "CALORIMETRY, Rheology and compressive strength of superplasticized cement pastes," *Cement and Concrete Research* **23**, 939-950 (1993).

18. S. H. Tantawi, "Effect of different types of concrete polymer admixtures on physicochemical and mechanical properties of cement pastes,"

Polymer-Plastics Technology and Engineering **36**, 863-872 (1997).

19. C. R. Wilding, "A combined conduction calorimeter and ultrasonic pulse velocity technique for monitoring the hydration setting of portland-cement," *Journal of Materials Science Letters* **3**, 13-14 (1984).

20. G. Dotelli and C. M. Mari, "The evolution of cement paste hydration process by impedance spectroscopy," *Materials Science and Engineering A-Structural Materials Properties Microstructure and Processing* **303**, 54-59 (2001).

21. P. Gu, V. S. Ramachandran, J. J. Beaudoin, and E. Quinn, "Electrochemical-behavior of portland-cement pastes containing phosphonates," *Advanced Cement Based Materials* **2**, 182-188 (1995).

22. J. Roncero, S. Valls, and R. Gettu, "Study of the influence of superplasticizers on the hydration of cement paste using nuclear magnetic resonance and X-ray diffraction techniques," *Cement and Concrete Research* **32**, 103-108 (2002).

23. Suput, J. S., Dimie, D., and Apih, T. Study of the influence of HRWR admixtures on the hydration processes of different types of portland cements by means of NMR spectroscopy. Cabrera, J. G. and Rivera-Villarreal, R. Proceedings of the International Symposium on the Role of Admmixtures in High Performance Concrete, 57-65. 1999. Bagneux, France, RILEM Publications. 3-21-1999.

24. S. A. FitzGerald, J. J. Thomas, D. A. Neumann, and R. A. Livingston, "A neutron scattering study of the role of diffusion in the hydration of tricalcium silicate," *Cement and Concrete Research* **32**, 409-413 (2002).

25. A. J. Allen, J. C. McLaughlin, D. A. Neumann, and R. A. Livingston, "In situ quasi-elastic scattering characterization of particle size effects on the hydration of tricalcium silicate," *Journal of Materials Research* **19**, 3242-3254 (2004).

26. J. J. Thomas, H. M. Jennings, and A. J. Allen, "Determination of the neutron scattering contrast of hydrated portland cement paste using H2O/D2O exchange," *Advanced Cement Based Materials* **7**, 119-122 (1998).

27. A. J. Allen, R. C. Oberthur, D. Pearson, P. Schofield, and C. R. WILDING, "Development of the Fine Porosity and Gel Structure of Hydrating Cement Systems," *Philosophical Magazine B-Physics of Condensed Matter Statistical Mechanics Electronic Optical and Magnetic Properties* **56**, 263-288 (1987).

28. D. N. Winslow, J. M. Bukowski, and J. F. Young, "The early evolution of the surface of hydrating cement," *Cement and Concrete Research* **24**, 1025-1032 (1994).

29. T. J. Chotard, A. Smith, D. Rotureau, D. Fargeot, and C. Gault, "Acoustic emission characterisation of calcium aluminate cement hydration at an early stage," *Journal of the European Ceramic Society* **23**, 387-398 (2003).

30. T. J. Chotard, M. P. Boncoeur-Martel, A. Smith, J. P. Dupuy, and C. Gault, "Application of X-ray computed tomography to characterise the early hydration of calcium aluminate cement," *Cement & Concrete Composites* **25**, 145-152 (2003).

31. A. Smith, T. Chotard, N. Gimet-Breart, and D. Fargeot, "Ultrasonic measurements as an in situ tool for characterising the ageing of an aluminous cement at different temperatures," *Journal of the European Ceramic Society* **22**, 2261-2268 (2002).

32. T. P. Philippidis and D. G. Aggelis, "An acousto-ultrasonic approach for the determination of water-to-cement ratio in concrete," *Cement and Concrete Research* **33**, 525-538 (2003).

33. D. G. Aggelis and T. P. Philippidis, "Ultrasonic wave dispersion and attenuation in fresh mortar," *Ndt & e International* **37**, 617-631 (2004).

34. J. R. Blakey, "Investigation of the percolation transition in hydrating cement using back-scattering methods," *Ultrasonics* **34**, 375-378 (1996).

35. T. Chotard, N. Gimet-Breart, A. Smith, D. Fargeot, J. P. Bonnet, and C. Gault, "Application of ultrasonic testing to describe the hydration of calcium aluminate cement at the early age," *Cement and Concrete Research* **31**, 405-412 (2001).

36. T. J. Chotard, J. Barthelemy, A. Smith, N. Gimet-Breart, M. Huger, D. Fargeot, and C. Gault, "Acoustic emission monitoring of calcium aluminate cement setting at the early age,"

Journal of Materials Science Letters **20**, 667-669 (2001).

37. T. J. Chotard, A. Smith, N. Gimet-Breard, M. Huger, D. Fargeot, and C. Gault, "Monitoring of calcium aluminate cement setting at the early age by acoustic emission technique," *Euro Ceramics Vii, Pt 1-3* **206-2**, 1851-1854 (2002).

38. T. J. Chotard, A. Smith, M. P. Boncoeur, D. Fargeot, and C. Gault, "Characterisation of early stage calcium aluminate cement hydration by combination of non-destructive techniques: acoustic emission and X-ray tomography," *Journal of the European Ceramic Society* **23**, 2211-2223 (2003).

39. B. Cros and J. Y. Ferrandis, "Characterization of the cement setting by acoustic near field," *Sensors and Actuators B-Chemical* **60**, 200-207 (1999).

40. B. Cros, A. Ramdani, and J. Y. Ferrandis, "Study of the setting of portland cement by an acoustic near field technique," *Revue de Metallurgie-Cahiers D Informations Techniques* **97**, 1525-+ (2000).

41. R. Dangelo, T. J. Plona, L. M. Schwartz, and P. Coveney, "Ultrasonic Measurements on Hydrating Cement Slurries - Onset of Shear-Wave Propagation," *Advanced Cement Based Materials* **2**, 8-14 (1995).

42. D. C. Darwin, R. Y. Leung, and T. Taylor, "Surface charge characterization of portland cement in the presence of superplasticizers," *SP 856, Electroacoustics for Characterization of Particulates and Suspensions,* S. G. Malghan, ed., (National Institute of Standards and Technology, Washington DC, 1993), 238-262.

43. J. Y. Ferrandis and G. Leveque, "In situ measurement of elastic properties of cement by an ultrasonic resonant sensor," *Cement and Concrete Research* **33**, 1183-1187 (2003).

44. R. J. Flatt and C. F. Ferraris, "Acoustophoretic characterization of cement suspensions," *Materials and Structures* **35**, 541-549 (2002).

45. N. Gimet, D. Fargeot, J. M. Gaillard, A. Smith, C. Gault, and J. P. Bonnet, "Ultrasonic assessment of portland cement at the early stages of hydration," *Journal of Materials Science Letters* **18**, 1335-1337 (1999).

46. H. C. Kim and S. S. Yoon, "Ultrasonic measurements during early-stage hydration of ordinary portland-cement," *Journal of Materials Science* **23**, 611-616 (1988).

47. H. K. Lee, K. M. Lee, Y. H. Kim, H. Yim, and D. B. Bae, "Ultrasonic in-situ monitoring of setting process of high-performance concrete," *Cement and Concrete Research* **34**, 631-640 (2004).

48. T. Ozturk, O. Kroggel, P. Grubl, and J. S. Popovics, "Improved ultrasonic wave reflection technique to monitor the setting of cement-based materials," *Ndt & e International* **39**, 258-263 (2006).

49. A. Ramdani, B. Cros, M. Sidki, and J. Y. Ferrandis, "Acoustic near field technique for characterization of liquids, bitumen and cement setting," *European Physical Journal-Applied Physics* **15**, 69-76 (2001).

50. J. R. Rapoport, J. S. Popovics, S. V. Kolluru, and S. P. Shah, "Using ultrasound to monitor stiffening process of concrete with admixtures," *Aci Materials Journal* **97**, 675-683 (2000).

51. C. M. Sayers and A. Dahlin, "Propagation of Ultrasound Through Hydrating Cement Pastes at Early Times," *Advanced Cement Based Materials* **1**, 12-21 (1993).

52. C. M. Sayers and R. L. Grenfell, "Ultrasonic propagation through hydrating cements," *Ultrasonics* **31**, 147-153 (1993).

53. A. Smith, T. Chotard, N. Gimet-Breart, and D. Fargeot, "Correlation between hydration mechanism and ultrasonic measurements in an aluminous cement: effect of setting time and temperature on the early hydration," *Journal of the European Ceramic Society* **22**, 1947-1958 (2002).

54. A. Smith, T. Chotard, J. P. Bonnet, F. Louvet, and C. Gault, "Ultrasonic characterization of model mixtures of hydrated aluminous cement," *Journal of Materials Science* **37**, 3847-3853 (2002).

55. J. Stepisnic, M. Lukac, and I. Kocuvan, "Measurement of Cement Hydration by Ultrasonics," *American Ceramic Society Bulletin* **60**, 481-483 (1981).

56. K. V. Subramaniam, J. P. Mohsen, C. K. Shaw, and S. P. Shah, "Ultrasonic technique for

monitoring concrete strength gain at early age," *Aci Materials Journal* **99**, 458-462 (2002).

57. Z. H. Sun, T. Voigt, and S. R. Shah, "Temperature effects on strength evaluation of cement-based materials with ultrasonic wave reflection technique," *Aci Materials Journal* **102**, 272-278 (2005).

58. R. Tatarin, W. Erfurt, and J. Stark, "Continuous ultrasonic investigations during the hydration of cement paste, mortar and concrete," *Zkg International* **57**, 69-78 (2004).

59. M. I. Valic, "Hydration of cementitious materials by pulse echo USWR: Method, apparatus and application examples," *Cement and Concrete Research* **30**, 1633-1640 (2000).

60. T. Voigt and S. P. Shah, "Properties of early-age portland cement mortar monitored with shear wave reflection method," *Aci Materials Journal* **101**, 473-482 (2004).

61. T. Voigt, G. Ye, Z. H. Sun, S. P. Shah, and K. van Breugel, "Early age microstructure of portland cement mortar investigated by ultrasonic shear waves and numerical simulation," *Cement and Concrete Research* **35**, 858-866 (2005).

62. T. Voigt, C. U. Grosse, Z. Sun, S. P. Shah, and H. W. Reinhardt, "Comparison of ultrasonic wave transmission and reflection measurements with P- and S-waves on early age mortar and concrete," *Materials and Structures* **38**, 729-738 (2005).

63. T. Voigt, Z. H. Sun, and S. P. Shah, "Comparison of ultrasonic wave reflection method and maturity method in evaluating early-age compressive strength of mortar," *Cement & Concrete Composites* **28**, 307-316 (2006).

64. G. Ye, K. van Breugel, and A. L. A. Fraaij, "Experimental study and numerical simulation on the formation of microstructure in cementitious materials at early age," *Cement and Concrete Research* **33**, 233-239 (2003).

65. G. Ye, P. Lura, K. van Breugel, and A. L. A. Fraaij, "Study on the development of the microstructure in cement-based materials by means of numerical simulation and ultrasonic pulse velocity measurement," *Cement & Concrete Composites* **26**, 491-497 (2004).

66. M. A. Biot, "Theory of Propagation of Elastic Waves in a Fluid-Saturated Porous Solid. II. Higher Frequency Range," *Journal of the Acoustical Society of America* **28**, 179-191 (1956).

67. M. A. Biot, "Theory of Propagation of Elastic Waves in a Fluid-Saturated Porous Solid. I. Low-Frequency Range," *Journal of the Acoustical Society of America* **28**, 168-178 (1956).

68. A. S. Dukhin and P. J. Goetz, "Acoustic and electroacoustic spectroscopy characterizing concentrated dispersions emulsions," *Advances in Colloid and Interface Science* **92**, 73-132 (2001).

69. D. J. Mcclements, "Ultrasonic Characterization of Emulsions and Suspensions," *Advances in Colloid and Interface Science* **37**, 33-72 (1991).

70. A. H. Harker and J. A. G. Temple, "Velocity and Attenuation of Ultrasound in Suspensions of Particles in Fluids," *Journal of Physics D-Applied Physics* **21**, 1576-1588 (1988).

71. J. R. Allegra and S. A. Hawley, "Attenuation of sound in suspensions and emulsions: theory and experiments," *Journal of the Acoustical Society of America* **51**, 1545-1564 (1972).

72. A. S. Dukhin and P. J. Goetz, "Acoustic spectroscopy for concentrated polydisperse colloids with high density contrast," *Langmuir* **12**, 4987-4997 (1996).

73. P. M. Morse and K. U. Ingard, *Theoretical acoustics*, (Princeton University Press, Princeton, N.J., 1986).

74. A. S. Dukhin and P. J. Goetz, *Ultrasound for characterizing colloids : particle sizing, zeta potential, rheology*, (Elsevier, Boston, 2002).

75. M. J. W. Povey, *Ultrasonic techniques for fluids characterization*, (; Academic Press, San Diego, 1997).

76. V. A. Hackley and J. Texter, *Ultrasonic and dielectric characterization techniques for suspended particulates*, (American Ceramic Society, Westerville, OH, 1998).

77. Information on CCRL and the proficiency program can be found at their web site: http://www.ccrl.us/.

78. E. J. Garboczi and J. W. Bullard, "Shape analysis of a reference cement," *Cement and Concrete Research* **34**, 1933-1937 (2004).

79. A. S. Dukhin and P. J. Goetz, "Acoustic and Electroacoustic Spectroscopy," *Handbook on Ultrasonic and Dielectric Characterization Techniques for Suspended Particulates,* V. A. Hackley and J. Texter, eds., (American Ceramic Society, Westerville OH, 1998), 77-95.

80. R. J. Hunter, "The Electroacoustic Characterization of Colloidal Suspensions," *Handbook on Ultrasonic and Dielectric Characterization Techniques for Suspended Particulates,* V. A. Hackley and J. Texter, eds., (American Ceramic Society, Westerville OH, 1998), 25-46.

81. V. A. Hackley, J. Patton, L.-S. H. Lum, R. J. Wasche, M. Naito, H. Abe, Y. Hotta, and H. Pendse, "Analysis of the Isoelectric Point in Moderately Concentrated Alumina Suspensions Using Electroacoustic and Streaming Potential Methods," *Journal of Dispersion Science and Technology* **23**, 601-617 (2002).

82. R. T. Klingbiel, H. Coll, R. O. James, and J. Texter, "Electrokinetic Sonic Amplitude of Colloidal Poly(methyl methacrylate) and Ludox-TM," *Colloids and Surfaces* **68**, 103-109 (1992).

83. A. S. Dukhin, P. J. Goetz, T. H. Wines, and P. Somasundaran, "Acoustic and electroacoustic spectroscopy," *Colloids and Surfaces A-Physicochemical and Engineering Aspects* **173**, 127-158 (2000).

Appendix A

Note: "#Labs" is the number of participating laboratories submitting results for proficiency testing. "S.D." is standard deviation and "C.V." is coefficient of variation.

CCRL PROFICIENCY SAMPLE PROGRAM
Portland Cement Proficiency Sample No. 133
Final Report - Chemical Results - September 17, 1999

SUMMARY OF RESULTS

Test		#Labs	Average	S.D.	C.V.
Silicon Dioxide	%	142	20.600	0.25	1.21
Aluminum Oxide (P_2O_5 & TiO_2 not included)	%	122	5.595	0.24	4.23
Ferric Oxide	%	141	2.485	0.058	2.35
Calcium Oxide	%	141	65.043	0.43	0.655
Free Lime	%	133	0.437	0.15	34.8
Magnesium Oxide	%	135	1.486	0.096	6.48
Sulfur Trioxide	%	147	2.308	0.066	2.86
Loss on Ignition	%	165	1.271	0.095	7.47
Insoluble Residue	%	156	0.222	0.065	29.5
Sodium Oxide	%	118	0.097	0.021	21.9
Potassium Oxide	%	124	0.606	0.022	3.62
Phosphorus Pent	%	57	0.096	0.011	12.0
Titanium Dioxide	%	63	0.354	0.020	5.64

CCRL PROFICIENCY SAMPLE PROGRAM
Portland Cement Proficiency Sample No. 133
Final Report - Physical Results - September 17, 1999

SUMMARY OF RESULTS

Test		#Labs	Average	S.D.	C.V.
N.C. Water	%	206	23.41	0.36	1.54
Vicat TS Initial	min	203	134.0	12.3	9.18
Vicat TS Final	min	197	227.6	30.1	13.2
Gillmore TS Initial	min	167	162.0	21.5	13.2
Gillmore TS Final	min	166	254.1	32.3	12.7
False Set	%	172	77.3	8.6	11.1
Autoclave Expan	%	197	0.005	0.018	362
Air Content	%	198	9.13	1.0	11.0
AC Mix Water	%	189	68.09	2.3	3.44
AC Flow	%	196	87.0	3.4	3.98
Comp Str 3-day	psi	214	3135.3	214.7	6.85
Comp Str 7-day	psi	212	4372.2	296.5	6.78
Comp Str 28-day	psi	178	5718.0	344.2	6.02
CS Flow	%	180	117.1	14.1	12.0
Fineness AP	sqcm/g	201	3488.8	70.0	2.0
Fineness WT	sqcm/g	34	1911.4	92.4	4.83
Passing 325 Sieve	%	189	86.966	1.23	1.41